

## Rare Control of SIVmac239 Infection in a Vaccinated Rhesus Macaque

Mauricio A. Martins,<sup>1</sup> Damien C. Tully,<sup>2</sup> Young C. Shin,<sup>1</sup> Lucas Gonzalez-Nieto,<sup>1</sup> Kim L. Weisgrau,<sup>3</sup>  
David J. Bean,<sup>2</sup> Rujuta Gadgil,<sup>2</sup> Martin J. Gutman,<sup>1</sup> Aline Domingues,<sup>1</sup> Helen S. Maxwell,<sup>1</sup>  
Diogo M. Magnani,<sup>1</sup> Michael Ricciardi,<sup>1</sup> Nuria Pedreño-Lopez,<sup>1</sup> Varian Bailey,<sup>1</sup> Michael A. Cruz,<sup>1</sup>  
Noemia S. Lima,<sup>4</sup> Myrna C. Bonaldo,<sup>4</sup> John D. Altman,<sup>5</sup> Eva Rakasz,<sup>3</sup> Saverio Capuano III,<sup>3</sup>  
Keith A. Reimann,<sup>6</sup> Michael Piatak Jr.,<sup>7,†</sup> Jeffrey D. Lifson,<sup>7</sup> Ronald C. Desrosiers,<sup>1</sup>  
Todd M. Allen,<sup>2</sup> and David I. Watkins<sup>1</sup>

### Abstract

Effector memory T cell ( $T_{EM}$ ) responses display potent antiviral properties and have been linked to stringent control of simian immunodeficiency virus (SIV) replication. Since recurrent antigen stimulation drives the differentiation of  $CD8^+$  T cells toward the  $T_{EM}$  phenotype, in this study we incorporated a persistent herpesviral vector into a heterologous prime/boost/boost vaccine approach to maximize the induction of  $T_{EM}$  responses. This new regimen resulted in  $CD8^+$   $T_{EM}$ -biased responses in four rhesus macaques, three of which controlled viral replication to  $<1,000$  viral RNA copies/ml of plasma for more than 6 months after infection with SIVmac239. Over the course of this study, we made a series of interesting observations in one of these successful controller animals. Indeed, *in vivo* elimination of  $CD8\alpha\beta^+$  T cells using a new  $CD8\beta$ -depleting antibody did not abrogate virologic control in this monkey. Only after its  $CD8\alpha^+$  lymphocytes were depleted did SIV rebound, suggesting that  $CD8\alpha\alpha^+$  but not  $CD8\alpha\beta^+$  cells were controlling viral replication. By 2 weeks postinfection (PI), the only SIV sequences that could be detected in this animal harbored a small in-frame deletion in *nef* affecting six amino acids. Deep sequencing of the SIVmac239 challenge stock revealed no evidence of this polymorphism. However, sequencing of the rebound virus following  $CD8\alpha$  depletion at week 38.4 PI again revealed only the six-amino acid deletion in *nef*. While any role for immunological pressure on the selection of this deleted variant remains uncertain, our data provide anecdotal evidence that control of SIV replication can be maintained without an intact  $CD8\alpha\beta^+$  T cell compartment.

**Keywords:** SIV vaccine, lymphocyte depletion, nonhuman primate, HIV/AIDS

### Introduction

**T**HE RATIONALE FOR ENGENDERING HIV-specific  $CD8^+$  T cell responses by vaccination comes from a wealth of data indicating that cellular immunity can limit viral replication *in vivo*.<sup>1–5</sup> While eliciting efficacious  $CD8^+$  T cells against this virus has not been straightforward, as evidenced

by the failures in clinical trials of all HIV-1 vaccine regimens aimed at inducing  $CD8^+$  T cell responses tested to date,<sup>6–8</sup> valuable insights have been gained from the simian immunodeficiency virus (SIV)/rhesus macaque model. For example, live-attenuated SIV vaccines have consistently afforded the greatest levels of efficacy against challenge with the pathogenic SIVmac239 clone.<sup>9,10</sup> Although protection in these

<sup>1</sup>Department of Pathology, University of Miami, Miami, Florida.

<sup>2</sup>Ragon Institute of MGH, MIT and Harvard, Cambridge, Massachusetts.

<sup>3</sup>Wisconsin National Primate Research Center, University of Wisconsin—Madison, Madison, Wisconsin.

<sup>4</sup>Laboratório de Biologia Molecular de Flavivirus, Instituto Oswaldo Cruz—FIOCRUZ, Rio de Janeiro, Brazil.

<sup>5</sup>Department of Microbiology and Immunology, Emory University, Atlanta, Georgia.

<sup>6</sup>MassBiologics, University of Massachusetts Medical School, Boston, Massachusetts.

<sup>7</sup>AIDS and Cancer Virus Program, Leidos Biomedical Research, Inc., Frederick National Laboratory for Cancer Research, Frederick, Maryland.

<sup>†</sup>Deceased.

cases is likely multifactorial, Fukazawa *et al.* have recently shown that the magnitude of effector-differentiated T cell responses in lymph nodes of vaccinated macaques correlates with the efficacy of live-attenuated SIV vaccines.<sup>10</sup> Importantly, the maintenance of these protective SIV-specific T cells correlated with the ability of live-attenuated SIV vaccines to persistently replicate at low levels in lymph nodes. By comparison, the majority of HIV/SIV vaccine platforms tested to date consist of weakened or replication-defective vectors that provide only transient antigen (Ag) exposure.<sup>11–14</sup> Although T cell responses elicited by these conventional vector platforms have often exhibited satisfactory immunogenicity profiles, their performance in stringent SIV challenge trials has varied considerably, ranging from no protection to partial virologic control.<sup>15–19</sup> Given the superior outcomes achieved with live-attenuated SIV vaccines, regimens that safely provide recurrent low-level exposure to viral proteins might facilitate the induction of effective antileviral T cell immunity.

Herpesviruses establish latent infections that persist for the life of the host.<sup>20</sup> Similar to live-attenuated SIV vaccination, herpesviral infections result in persistent Ag stimulation, which favors the induction of effector memory T cell ( $T_{EM}$ ) responses.<sup>21</sup> This phenotype is associated with T cells that recirculate through extralymphoid tissues and are poised for immediate antiviral activity.<sup>22</sup> The persistent nature of herpesviruses and the antiviral properties of  $T_{EM}$  prompted the generation of live recombinant (r) herpesviral vectors encoding SIV proteins. For example, a fibroblast-adapted strain of the  $\beta$ -herpesvirus rhesus cytomegalovirus (RhCMV) expressing SIV inserts has shown great promise in monkey trials with approximately half of RhCMV/SIV vaccinees manifesting early and profound control of viral replication after SIVmac239 infection.<sup>23,24</sup> Remarkably, these protected vaccinees eventually cleared SIV *in vivo*, implying that lentiviral infections are vulnerable to early interception by vaccine-induced  $T_{EM}$  responses.<sup>25</sup> Importantly, RhCMV is not the only herpesviral vector platform available for persistent Ag delivery in nonhuman primates. In fact, a genetic system for the  $\gamma$ 2-herpesvirus rhesus monkey rhadinovirus (RRV) has also been developed,<sup>26</sup> facilitating the generation of rRRV/SIV vectors.<sup>27</sup> In contrast to the unconventionally major histocompatibility complex (MHC)-restricted  $CD8^+$   $T_{EM}$  responses elicited by the aforementioned RhCMV strain,<sup>28,29</sup> rRRV/SIV-vaccinated macaques develop  $CD8^+$  T cells capable of recognizing classically immunodominant MHC class I-restricted SIV epitopes.<sup>27</sup> Following intravenous challenge with SIVmac239, rRRV/SIV vaccinees manifested significant reductions in peak and set point viremia compared to unvaccinated controls. Collectively, these data highlight the utility of herpesviral vectors for eliciting lentivirus-specific  $T_{EM}$  responses.

Repeated Ag stimulation delivered in the form of heterologous prime/boost/boost (PBB) immunization protocols has been shown to generate robust  $CD8^+$   $T_{EM}$  responses in mice.<sup>30,31</sup> Similarly, we have recently shown that a rDNA prime followed by boosting with rYF17D and rAd5 resulted in high-frequency SIV-specific  $T_{EM}$  responses in rhesus macaques.<sup>32</sup> However, these vaccine-induced  $CD8^+$  T cells underwent considerable contraction soon after the rAd5 boost, possibly due to the lack of persistent Ag stimulation afforded by the rDNA/rYF17D/rAd5 protocol. In an attempt to improve the maintenance of  $CD8^+$   $T_{EM}$  responses, we delivered a final rRRV/SIV boost to four rhesus macaques that had been im-

munized with an rDNA prime followed by a rYF17D boost. In addition to evaluating the immunogenicity and efficacy of this new rDNA/rYF17D/rRRV regimen, this pilot study resulted in an extraordinary outcome in one of the vaccinated monkeys. Using viral sequencing and selective depletions of  $CD8\beta$ - or  $CD8\alpha$ -expressing lymphocytes *in vivo*, we investigated immunological and virologic aspects of this rare case of control of SIVmac239 replication.

## Materials and Methods

### Research animals

The four Indian rhesus macaques used in the vaccine pilot study described in Figure 1 were naturally infected with RRV. The two SIV-infected Indian rhesus macaques used in the experiment described in Figure 4 were part of a recent study conducted by our laboratory and were used to further characterize the effects of  $CD8\beta$  depletion during controlled SIV infection. All animals were housed at the Wisconsin National Primate Research Center (WNPRC) and cared for in accordance with the Weatherall Report under a protocol approved by the University of Wisconsin Graduate School Animal Care and Use Committee. Vaccinations, SIV challenges, and monoclonal antibody (mAb) infusions were performed under anesthesia, and all efforts were made to minimize potential suffering. Additional animal information, including MHC class I alleles, age, and sex, is shown in Table 1.

### Vaccinations

The macaques in Groups 1 and 2 were primed once with rDNA plasmids expressing SIVmac239 minigenes encoding Nef amino acids (aa) 45–210 (Group 1) or Gag aa 178–258 (Group 2). One milligram of each rDNA/SIV vector and 0.1 mg of an IL-12-expressing plasmid were codelivered by intramuscular electroporation. The monkeys then received 300,000 plaque-forming units of rYF17D vectors encoding the same inserts as the rDNA plasmids through the subcutaneous route. Additional information on the rDNA and rYF17D vaccinations can be found elsewhere.<sup>33</sup> The third and last vaccine boost consisted of a single infusion of 1.0 mL of phosphate-buffered saline (PBS) solution containing  $7.0 \times 10^8$  genome copies of rRRV vectors encoding SIVmac239 inserts. Animals in Group 1 received rRRV/*rev-tat-nef* while those in Group 2 were vaccinated with rRRV/*gag* (Fig. 1A). The construction of these rRRV/SIV vaccines has been described elsewhere.<sup>27</sup>

TABLE 1. ANIMAL CHARACTERISTICS

Experimental group	Animal ID	MHC-I alleles	Age (year) <sup>a</sup>	Gender
Group 1	r04132	<i>Mamu-B*08</i>	8.3	Female
	r07032	<i>Mamu-B*08</i>	5.3	Male
Group 2	r08019	<i>Mamu-A*01</i>	4.7	Female
	r01049	<i>Mamu-A*01</i>	11.7	Male
Group 3	r09037	<i>Mamu-B*08</i>	6.2	Female
	r09089	<i>Mamu-B*08</i>	5.8	Male

<sup>a</sup>Animal age at the beginning of study.  
MHC, major histocompatibility complex.

### *SIV<sub>mac239</sub> challenges*

The challenge stock utilized in this study was produced by the Virology Services Unit of the WNPRC using SIV<sub>mac239</sub> hemi-genome plasmids obtained from the NIH AIDS Research and Reference Reagent Program. These plasmids were transfected into 293T cells, and the supernatant was propagated on mitogen-activated peripheral blood mononuclear cell (PBMC) from SIV naive rhesus macaques for several days. The titer of this stock was 90,000 50% tissue culture infective doses (TCID<sub>50</sub>)/mL. Animals in this study were subjected to the same weekly intrarectal (IR) SIV<sub>mac239</sub> challenge regimen described recently.<sup>32</sup> The dose of each exposure was 200 TCID<sub>50</sub>, which corresponded to  $4.8 \times 10^5$  viral RNA (vRNA) copies. Plasma viral loads (VLs) were assessed 3 and 7 days after each exposure. Once an animal had a positive VL, it was no longer challenged.

### *In vivo CD8 depletions*

CD8 $\beta$ -expressing lymphocytes were transiently depleted using the anti-CD8 $\beta$  mAb CD8 $\beta$ 255R1. The parental mouse mAb was raised against rhesus CD8 $\beta$  chain and engineered into a recombinant rhesus IgG1 by complementarity determining region (CDR) grafting. CD8 $\alpha^+$  cells were depleted using a CDR-grafted rhesus IgG1, MT807R1, derived from a mouse anti-human CD8 $\alpha$  mAb.<sup>34</sup> All animals were administered a single intravenous injection of 50 mg/kg of body weight. Both mAbs were provided by the NIH Nonhuman Primate Reagent Resource (Boston, MA).

### *MHC class I tetramer staining and immunophenotyping during lymphocyte depletions*

We monitored the ontogeny of vaccine-induced SIV-specific CD8 $^+$  T cell responses in Groups 1 and 2 using fluorochrome-labeled MHC class I tetramers, as described recently.<sup>35</sup> In sum, PBMCs were isolated from blood drawn at the WNPRC on the previous day and then shipped to the University of Miami overnight. We used allophycocyanin-conjugated Mamu-B\*08/Nef<sub>137-146</sub>RL10 (NIH Tetramer Core Facility) and Mamu-A\*01/Gag<sub>181-189</sub>CM9 (MBL International) tetramers to monitor vaccine-induced SIV-specific CD8 $^+$  T cell responses in the Group 1 and Group 2 macaques, respectively. Up to 800,000 PBMCs were incubated with titrated amounts of each tetramer at 37°C for 1 h and then stained with fluorochrome-labeled antibodies directed against the surface molecules CD3 (clone SP34-2), CD8 $\alpha$  (clone RPA-T8), CD28 (clone 28.2), CCR7 (clone 150503), CD14 (clone M5E2), CD16 (clone 3G8), and CD20 (clone 2H7). Amine-reactive dye (ARD; LIVE/DEAD Fixable Aqua Dead Cell Stain; Life Technologies) was also added to this mAb cocktail. After a 25-min incubation at room temperature (RT), the cells were washed with Wash Buffer (Dulbecco's PBS with 0.1% bovine serum albumin and 0.45 g/L NaN<sub>3</sub>) and then fixed with PBS containing 2% of paraformaldehyde. The configuration of the Special Order Product BD LSR II cytometer used to acquire the samples and the gating strategy used to analyze the data have been detailed elsewhere.<sup>32</sup> In sum, we used FlowJo 9.6 to determine the percentages of live CD14 $^-$ CD16 $^-$ CD20 $^-$ CD3 $^+$ CD8 $^+$ tetramer $^+$  lymphocytes displayed on Figure 1B, C and to delineate memory subsets within tetramer $^+$  populations (Fig. 1D, E).

To monitor the frequencies of lymphocyte subsets during the CD8 $\beta$  and CD8 $\alpha$  depletions, our surface staining master mix included the same clones of anti-CD3, anti-CD14, anti-CD16, and anti-CD20 antibodies and the same ARD reagent mentioned above. In addition, this cocktail included antibodies against the CD8 $\alpha$  chain (clone SK1 for the CD8 $\beta$  depletion phase or clone DK25 for the CD8 $\alpha$  depletion phase) and the CD8 $\alpha\beta$  heterodimer (clone 2ST8-5H7). This latter clone recognizes a conformational epitope consisting of domains from both the CD8 $\alpha$  and CD8 $\beta$  chains.<sup>36</sup> Of note, the CD8 glycoprotein can be expressed as two isoforms: CD8 $\alpha\beta$  heterodimers or CD8 $\alpha\alpha$  homodimers.<sup>37</sup> The anti-CD8 $\alpha$  mAb MT807R1 that was used to deplete CD8 $\alpha^+$  lymphocytes *in vivo* is known to cross-block other anti-CD8 antibodies used for immunophenotyping. However, the anti-CD8 $\alpha$  clone DK25 can still resolve CD8 $\alpha^+$  cells in the presence of MT807R1, although with reduced fluorescence intensity.<sup>34</sup> In quality assessment tests performed in our laboratory, we found that preincubation of PBMC with 50  $\mu$ g/mL of the anti-CD8 $\beta$  mAb CD8 $\beta$ 255R1 did not prevent fluorochrome-labeled 2ST8-5H7 antibodies from detecting CD8 $\alpha\beta^+$  T cells, although there was a slight reduction in fluorescence intensity (data not shown). In contrast, preincubation of PBMC with 50  $\mu$ g/mL of MT807R1 completely blocked staining with 2ST8-5H7. During the CD8 $\beta$  depletion phase, CD3 $^+$  T lymphocytes that were positive for CD8 $\alpha$  but negative for CD8 $\alpha\beta$  were considered to be CD8 $\alpha\alpha^+$ . To obtain relative frequencies of lymphocyte subsets, we first excluded monocytes, B cells, and dead cells in the "dump gate" (CD14 $^+$ CD20 $^+$ ARD $^+$ ) and then determined the percentages of CD8 $\alpha\beta^+$  T cells (CD3 $^+$ CD8 $\alpha\alpha^-$ CD8 $\alpha\beta^+$ ), CD8 $\alpha\alpha^+$  T cells (CD3 $^+$ CD8 $\alpha\alpha^+$ CD8 $\alpha\beta^-$ ), CD4 $^+$  T cells (considered as CD3 $^+$ CD8 $\alpha\alpha^-$ CD8 $\alpha\beta^-$ ), and NK cells (CD3 $^-$ CD8 $\alpha\alpha^+$ CD16 $^+$ ) within the lymphocyte gate. Absolute counts of these subsets were then calculated by multiplying their respective frequencies by the absolute number of white blood cells obtained from matching complete blood counts.

### *Intracellular cytokine staining assay*

The intracellular cytokine staining (ICS) assay was performed as described recently.<sup>32</sup> In sum, cells were stimulated with SIV peptides at a final concentration of 1.0  $\mu$ M in the presence of costimulatory mAbs against CD28 (clone L293; BD Biosciences) and CD49d (clone 9F10; BD Pharmingen) for 9 h at 37°C in a 5.0% CO<sub>2</sub> incubator. To inhibit protein transport, Brefeldin A (BioLegend, Inc.) and GolgiStop (BD Biosciences) were added to all tubes 1 h into the incubation period. We used the same steps outlined above to stain molecules on the surface of cells and to fix them with 2% of paraformaldehyde. In addition to the same mAbs against CD14, CD16, and CD20 and the ARD reagent described above, the surface staining master mix also included mAbs against CD4 (clone OKT4; BioLegend, Inc.) and CD8 (clone RPA-T8; BioLegend, Inc.). Cells were permeabilized by resuspending them in "Perm Buffer" [1 $\times$ BD FACS lysing solution 2 (Becton Dickinson) and 0.05% Tween 20 (Sigma-Aldrich)] for 10 min and subsequently washed with Wash Buffer. Cells were then incubated with mAbs against IFN- $\gamma$  (clone 4S.B3; BioLegend, Inc.), TNF- $\alpha$  (clone Mab11; BD Biosciences), and CD3 (same one mentioned above) for 1 h in the dark at RT, washed, and subsequently stored at 4°C until acquisition.

### Anti-immunoglobulin enzyme-linked immunosorbent assay

Enzyme-linked immunosorbent assay (ELISA) plates (Nunc-Immuno) were coated overnight at 4°C with either MT807R1 or CD8 $\beta$ 255R1. All subsequent steps and incubations were performed at RT. On the following day, plates were washed five times with Wash Buffer (PBS containing 0.05% of Tween 20) and then blocked with SuperBlock buffer (Thermo Scientific) for 15 min. Plasma from r04132 and r08019 collected 8 days before (predepletion) or 22 days after (postdepletion) the anti-CD8 $\beta$  mAb infusion was used in this assay. Plasma from untreated or anti-CD8 $\alpha$ -treated monkeys was used as negative and positive controls, respectively. After diluting plasma samples 10-fold in PBS containing 2% of bovine serum albumin, these aliquots were serially diluted 1:4 until a dilution factor of 10,240 was achieved. One hundred microliters of these serially diluted plasma aliquots were added to plates, followed by a 1-h incubation. Subsequently, plates were washed five times, and 100  $\mu$ L of a 100-fold dilution of anti-immunoglobulin (Ig) human  $\lambda$  light chain conjugated to biotin (Miltenyi Biotec) was added to each well and incubated for 1 h. Plates were then washed five times before 100  $\mu$ L of a 10,000-fold dilution of horseradish peroxidase-conjugated Streptavidin (Invitrogen) was added to each well. After a 1-h incubation, plates were washed five times. One hundred microliters of TMB (Calbiochem) was added to the plates for  $\sim$ 3 min and then the substrate reaction was stopped with H<sub>2</sub>SO<sub>4</sub> Stop Solution (Southern Biotech). The optical density (OD) of each well was determined on an ELISA reader using a 450 nm filter. End point titers of anti-Ig antibodies were considered as the highest dilutions where the OD of the postdepletion sample was >2-fold higher than its predepletion counterpart.

### SIV VL measurements

VLs were measured using 0.5 mL of EDTA-anticoagulated plasma based on a modification of a previously published protocol.<sup>38</sup> Total RNA was extracted from plasma samples using QIAgen DSP virus/pathogen Midi kits, on a QIASymphonyXP laboratory automation instrument platform. Six replicate two-step reverse transcription-polymerase chain reaction (RT-PCR) were performed per sample using a random primed reverse transcription reaction, followed by 45 cycles of polymerase chain reaction (PCR) using the following primers and probe: forward primer: SGAG21: 5'-GTCTGCGTCAT(dP)TGGTGCATTC-3'; reverse primer SGAG22: 5'-CACTAG(dK)TGTCTCTGCACTAT(dP)TGT TTTG-3'; probe: PSGAG23: 5'-FAM-CTTC(dP)TCAGT(dK)TGTTCACTTTCTCTTCTGCG-BHQ1-3'. The limit of reliable quantitation on an input volume of 0.5 mL of plasma was 15 vRNA copies/ml.

### Whole-genome deep sequencing of SIVmac239

vRNA in plasma was isolated using the QIAamp vRNA Mini Kit (QIAGEN), according to the manufacturer's protocol, and eluted in 60  $\mu$ L of AVE buffer. The eluate was then aliquoted and stored at -80°C for future use. vRNA was reverse transcribed and amplified using the SuperScript III One-Step RT-PCR system with High Fidelity Platinum Taq polymerase (Invitrogen). PBMCs from rhesus macaque were

washed twice with PBS, and DNA was then extracted from the cells using the QIAamp DNA Blood Mini Kit (QIAGEN) with PCR amplifications performed as described below with the exception of the first RT step. For the r08019 week 38.4 postinfection (PI) sample, a near full-length genome of SIV was amplified in four segments using the following primers: Amp1-F (5'-AGGAACCAACCACGACGGAG-3') and Amp1-R (5'-AAAGGGATTGGCACTGGTGGCAGG-3'); Amp2-F (5'-TGCTGACGGCTTGTCAAGGAGTAGG-3') and Amp2-R (5'-ACCCTGTCATGTTCCAGGTCTGTCC-3'); Amp3-F (5'-ATGGTGGCAGGGATAGAGC-3') and Amp3-R (5'-CCATGCCTGCTTTGGCCTAT-3'); and Amp4-F (5'-TGCA CAGGCTTGGAAACAAGA-3') and Amp4-R (5'-ACATC CCCTTGTGGAAAGTC-3'). The RT-PCR conditions were as follows for Amp 1 and 2: 50°C for 30 min; 94°C for 2 min; 40 cycles of 94°C for 15 s, 55°C for 30 s, and 68°C for 3 min; and 68°C for 5 min and for Amp 3 and 4: 45°C for 120 min, 94°C for 15 s; 40 cycles of 94°C for 15 s, 50°C for 30 s, and 68°C for 6 min; and 68°C for 6 min. In the case of PBMC from r08019 collected at week 2 PI, only one amplicon was successfully amplified and sequenced, despite multiple attempts using different primer sets and conditions. A 2.4-kb fragment spanning part of *env* and *nef* (positions 7,565–9,979) amplified using forward primer (5'-CAGTCACCA TTATGTCTGGATTG-3') and reverse primer (5'-GAATAC AGAGCGAAATGCAGTG-3') under the conditions detailed above for amp 1 and 2. A smaller amplicon-based 454 sequencing approach was used to analyze a 400-bp region in *Nef* as previously described.<sup>39</sup> Whole genome deep sequencing was also performed on the SIVmac239 challenge as previously described.<sup>40</sup>

Amplicons were visualized on a 1.0% agarose gel and purified using the PureLink Quick Gel Extraction Kit (Invitrogen). RT-PCR products were quantified using a Promega QuantiFluor-ST fluorometer (Promega) and analyzed for quality using an Agilent 2100 Bioanalyzer with high sensitivity DNA chips. PCR amplicons were fragmented and bar coded using Nextera XT DNA Library Prep Kit, as per manufacturer's protocol. Samples were pooled and sequenced on an Illumina MiSeq platform, using a 2  $\times$  250-bp V2 Reagent Kit. Paired-end reads obtained from Illumina MiSeq were assembled into a SIV consensus sequence using the VICUNA *de novo* assembler software and finished with V-FAT v1.0.<sup>41</sup> Reads were mapped back to this consensus using Mosaik v2.1.73 and intrahost variants called by V-Phaser v2.0.<sup>42,43</sup> All reads have been deposited to the NCBI Sequence Read Archive under accession number SRP016012.

### Results

Four rhesus macaques were equally divided between two groups based on their MHC class I alleles: monkeys in Group 1 were *Mamu-B\*08*<sup>+</sup> and those in Group 2 were *Mamu-A\*01*<sup>+</sup> (Fig. 1A). We chose these MHC class I alleles because their gene products present immunodominant SIV epitopes. Specifically, *Mamu-B\*08* binds to Nef<sub>137-146</sub>RL10, while *Mamu-A\*01* restricts Gag<sub>181-189</sub>CM9.<sup>44,45</sup> Of note, expression of *Mamu-B\*08* has been linked to elite control of SIVmac239 infection.<sup>46</sup>

To achieve the continual Ag stimulation that favors induction of T<sub>EM</sub> responses,<sup>21,47</sup> we combined the repetitive boosting provided by heterologous PBB regimens and the

persistent Ag exposure afforded by herpesviral infections into a new immunization protocol. This protocol consisted of successive vaccinations with electroporated rDNA, rYF17D, and rRRV vectors encoding SIV<sub>mac239</sub> inserts (Fig. 1A). The vectors used in Group 1 and Group 2 delivered the Nef<sub>137-146</sub>RL10 and Gag<sub>181-189</sub>CM9 epitopes, respectively, to match the expressed MHC class I alleles (Fig. 1A). To monitor the ontogeny of vaccine-induced CD8<sup>+</sup> T cell responses against each epitope, we performed longitudinal fluorochrome-labeled MHC class I tetramer stainings in PBMC from the Group 1 and Group 2 animals. The two Mamu-B\*08<sup>+</sup> vaccinees developed low frequency responses against Nef<sub>137-146</sub>RL10, with percentages of tetramer<sup>+</sup>CD8<sup>+</sup> T cells peaking at 4% and then decreasing to <1% of CD8<sup>+</sup> T cells by week 34 post rYF17D (Fig. 1B). Conversely, both Mamu-A\*01<sup>+</sup> animals in Group 2 mounted robust Gag<sub>181-189</sub>CM9-specific CD8<sup>+</sup> T cells after the rRRV boost (14% and 16% at peak; Fig. 1C). While the magnitude of these tetramer<sup>+</sup>CD8<sup>+</sup> T cells eventually declined to <1% in r01049, the other Group 2 vaccinee (r08019) maintained its Gag<sub>181-189</sub>CM9-specific response at 4.6% after resolution of the peak response (Fig. 1C). It is not entirely clear why the contraction of vaccine-induced SIV-specific CD8<sup>+</sup> T cells was accentuated in both Group 1 animals and in r01049 in the weeks following the rRRV boost. Given that captive rhesus monkeys can be naturally infected with RRV,<sup>48,49</sup> preexisting immunity to this herpesvirus may have limited the “take” of the live rRRV vectors utilized in this study. Indeed, all four monkeys in Groups 1 and 2 were seropositive for RRV at the time of the rRRV vaccination (data not shown).

We also carried out a phenotypic analysis of vaccine-induced SIV-specific CD8<sup>+</sup> T cells at week 34 post rYF17D

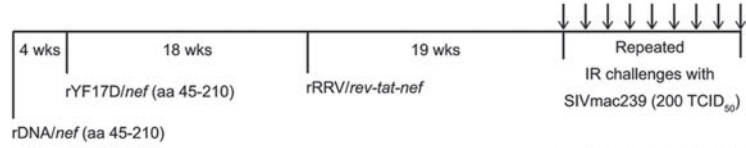
and found a predominance of the fully differentiated T<sub>EM2</sub> (CD28<sup>+</sup>CCR7<sup>-</sup>) phenotype (Fig. 1D, E), indicative of persistent Ag stimulation. Transitional memory (T<sub>EM1</sub>; CD28<sup>+</sup>CCR7<sup>+</sup>) and central memory (T<sub>CM</sub>; CD28<sup>+</sup>CCR7<sup>+</sup>) tetramer<sup>+</sup>CD8<sup>+</sup> T cells were also detected, especially in the Group 1 vaccinee r04132 (Fig. 1D). In sum, while 3/4 vaccinees had low frequencies of SIV-specific CD8<sup>+</sup> T cells at the time of SIV challenge, r08019 was clearly an outlier since >4% of its peripheral CD8<sup>+</sup> T cell compartment was specific for a single SIV epitope and 96% of these exhibited the T<sub>EM2</sub> phenotype.

At week 19 post rRRV boost, we began challenging all animals intrarectally with 200 TCID<sub>50</sub> of an *in vivo*-titrated SIV<sub>mac239</sub> stock. Of note, out of the 32 SIV naive rhesus macaques that have been subjected to this IR challenge regimen (same viral stock and dose) as part of ongoing experiments conducted by our group, 78% became infected by the sixth exposure (Martins *et al.*, unpublished observations). Remarkably, after becoming infected after the ninth IR challenge (Fig. 1F), the Group 2 vaccinee r08019 experienced a peak VL of only 1,000 vRNA copies/ml of plasma and subsequently controlled viremia to <15 vRNA copies/ml by week 5 PI (Fig. 1G). In contrast, the other Group 2 animal (r01049) became infected after the fifth challenge and failed to suppress viremia (Fig. 1F, G). Encouragingly, both Group 1 vaccinees had relatively low peak VLs and controlled chronic phase VLs to <1,000 vRNA copies/ml (Fig. 1G). As a reference, we compared VLs in Groups 1 and 2 with those from MHC class I-matched macaques that were rectally infected with SIV<sub>mac239</sub> as part of previous and ongoing studies conducted by our laboratory (Martins *et al.*, unpublished observations).<sup>32,33,39</sup> These historical controls

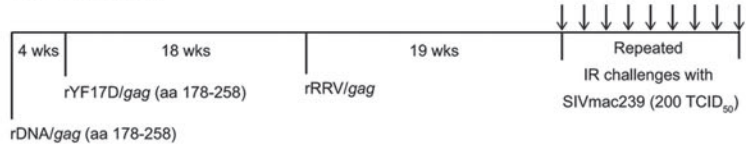
**FIG. 1.** Design, immunogenicity, and efficacy of an rDNA/rYF17D/rRRV regimen encoding immunodominant classical CD8<sup>+</sup> T cell epitopes. (A) Two Mamu-B\*08<sup>+</sup> (Group 1) and two Mamu-A\*01<sup>+</sup> (Group 2) Indian rhesus macaques were immunized with a heterologous prime/boost/boost vaccine regimen aimed at eliciting high frequency CD8<sup>+</sup> T<sub>EM</sub> responses against immunodominant SIV determinants. These animals were primed once with rDNA delivered by intramuscular electroporation followed by two viral vector boosts with rYF17D and then rRRV. Both the rDNA plasmids and the rYF17D encoded SIV<sub>mac239</sub> minigenes corresponding to aa 45-210 of the Nef protein (Group 1) or aa 178-258 of the Gag polypeptide (Group 2). The rRRV vectors expressed a *rev-tat-nef* fusion (Group 1) or full-length *gag* (Group 2). Of note, all macaques in Groups 1 and 2 were seropositive for RRV at the time of the rRRV vaccinations. In keeping with the animals' expressed MHC class I genotypes, macaques in Group 1 received inserts encoding the Mamu-B\*08-restricted Nef<sub>137-146</sub>RL10 epitope, while those in Group 2 were vaccinated with *gag* sequences containing the Mamu-A\*01-restricted Gag<sub>181-189</sub>CM9 determinant. Nineteen weeks following the rRRV boost, we began challenging the Group 1 and Group 2 monkeys every week with IR inoculations of 200 TCID<sub>50</sub> of an *in vivo*-titered SIV<sub>mac239</sub> stock.<sup>32</sup> (B, C) Vaccine-induced SIV-specific CD8<sup>+</sup> T cell responses in Group 1 (B) and Group 2 (C). We monitored the ontogeny of vaccine-elicited CD8<sup>+</sup> T cell responses in Groups 1 and 2 by staining PBMC with fluorochrome-labeled Mamu-B\*08/Nef<sub>137-146</sub>RL10 and Mamu-A\*01/Gag<sub>181-189</sub>CM9 tetramers, respectively. Only time points following the rYF17D boost are displayed. The last measurement was performed at week 34 post rYF17D vaccination, 3 weeks before the first IR challenge with SIV<sub>mac239</sub>. (D, E) Memory phenotype of vaccine-induced CD8<sup>+</sup> T cells in Group 1 (D) and Group 2 (E) at week 34 post rYF17D vaccination. Based on the expression of CD28 and CCR7, tetramer<sup>+</sup>CD8<sup>+</sup> T cells in PBMC were classified as fully differentiated effector memory (T<sub>EM2</sub>; CD28<sup>+</sup>CCR7<sup>-</sup>), transitional memory (T<sub>EM1</sub>; CD28<sup>+</sup>CCR7<sup>+</sup>), or central memory (T<sub>CM</sub>; CD28<sup>+</sup>CCR7<sup>+</sup>) subsets. (F) Rate at which macaques in Groups 1 and 2 became infected following repeated IR challenges with SIV<sub>mac239</sub>. The frequency of each animal's tetramer<sup>+</sup>CD8<sup>+</sup> T cells at week 34 post rYF17D is shown as a reference. (G) Log-transformed VLs after SIV<sub>mac239</sub> infection. The *dashed line* in the graph is for reference only and indicates a VL of 10<sup>6</sup> vRNA copies/ml. The *dotted line* is also for reference only and denotes a VL of 10<sup>3</sup> vRNA copies/ml. The limit of reliable quantitation of this VL assay was 15 vRNA copies/ml of plasma. To assess the extent to which vaccinees in Groups 1 and 2 decreased plasma viremia, geometric means of VLs measured in unvaccinated MHC class I-matched macaques that were rectally infected with SIV<sub>mac239</sub> as part of current and recent studies conducted in our laboratory are also plotted (Martins *et al.*, unpublished observations).<sup>32,33,39</sup> These geometric means were calculated based on VLs measured within weeks 1–20 PI in 12 Mamu-B\*08<sup>+</sup> and 8 Mamu-A\*01<sup>+</sup> macaques. IR, intrarectal; MHC, major histocompatibility complex; PI, postinfection; PBMC, peripheral blood mononuclear cell; RRV, rhadinovirus; SIV, simian immunodeficiency virus; T<sub>EM</sub>, effector memory T cell; VL, viral load; vRNA, viral RNA.

**A** Experimental layout

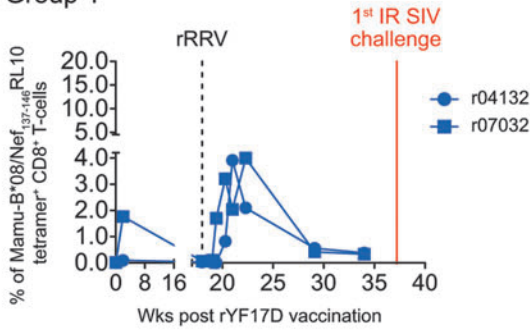
**Group 1**  
All Mamu-B\*08\*



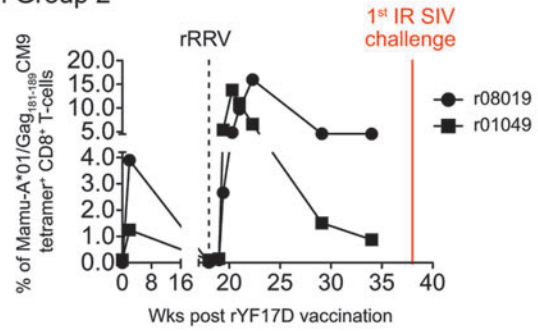
**Group 2**  
All Mamu-A\*01\*



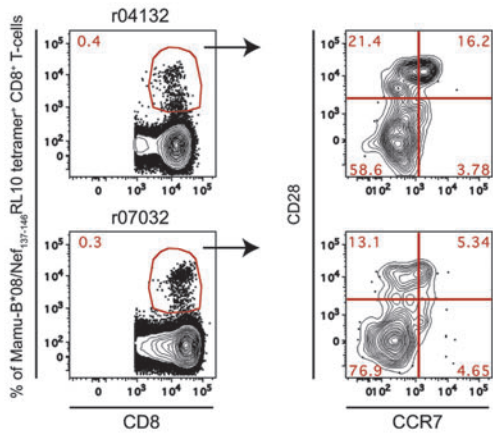
**B** Vaccine-induced CD8<sup>+</sup> T-cell responses in Group 1



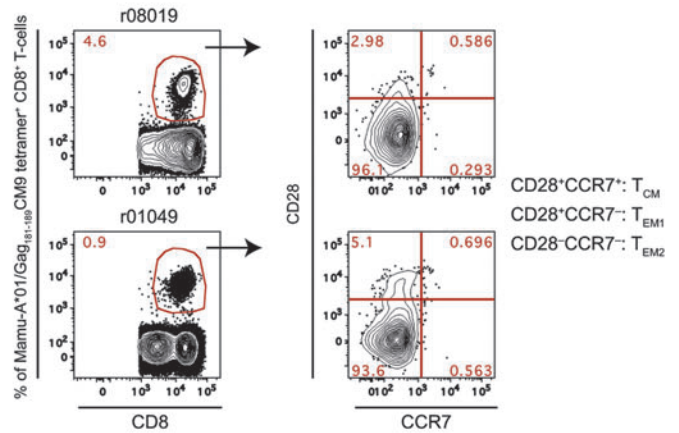
**C** Vaccine-induced CD8<sup>+</sup> T-cell responses in Group 2



**D** Memory phenotype of vaccine-induced CD8<sup>+</sup> T-cells in Group 1



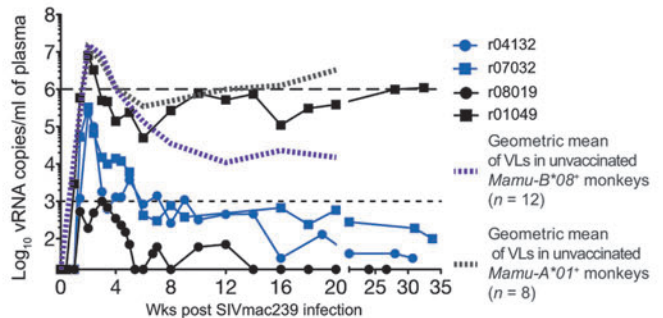
**E** Memory phenotype of vaccine-induced CD8<sup>+</sup> T-cells in Group 2



**F** Rate of SIV acquisition

Animal ID	% of tetramer <sup>+</sup> CD8 <sup>+</sup> T-cells at wk 34 post rYF17D	Infecting IR exposure								
		1	2	3	4	5	6	7	8	9
r04132	0.4					X				
r07032	0.3		X							
r01049	0.9					X				
r08019	4.6									X

**G** Viral loads





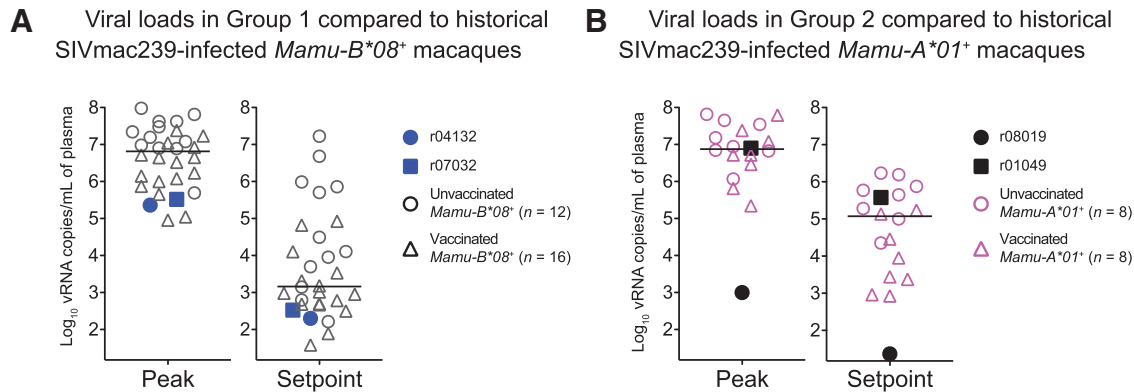


**FIG. 2.** Peak and set point VLs in Groups 1 and 2 compared to historical SIVmac239-infected macaques. **(A)** Log-transformed peak and set point VLs in r04132 and r07032 were plotted alongside the same VL values from *Mamu-B\*08*<sup>+</sup> rhesus macaques that were rectally infected with SIVmac239 as part of ongoing and recent studies conducted in our laboratory (Martins *et al.*, unpublished observations).<sup>32,33,39</sup> Each symbol corresponds to one monkey. For this analysis, unvaccinated macaques ( $n=12$ ) are denoted by *open circles*, whereas vaccinated monkeys ( $n=16$ ) are denoted by *open triangles*. **(B)** Peak and set point VLs in r08019 and r10149 are displayed alongside VLs from SIVmac239-infected, *Mamu-A\*01*<sup>+</sup> rhesus macaques. As in **A**, *open circles* correspond to unvaccinated monkeys ( $n=8$ ), whereas *open triangles* indicate vaccinated animals ( $n=8$ ). In all cases, set point was determined as the geometric mean of VLs measured between week 6 PI and the last available postinfection time point. Bars correspond to medians.

included both unvaccinated and vaccinated monkeys (Fig. 2). Overall, the two Group 1 vaccinees experienced lower peak and set point VLs than the majority of their *Mamu-B\*08*<sup>+</sup> historical counterparts while r08019 exhibited the lowest levels of viremia among our cohort of *Mamu-A\*01*<sup>+</sup> historical controls (Fig. 2). Thus, a rDNA/rYF17D/rRRV regimen encoding immunodominant SIV epitopes resulted in stringent control of SIVmac239 replication in 3/4 vaccinees.

Given r08019's remarkable outcome, we then explored several potential mechanisms for the impressive virologic control observed in this animal. First, we postulated that this animal's robust vaccine-induced SIV-specific CD8<sup>+</sup> T cell response was responsible for containing viral replication. Based on this assumption and on our previous experimental data,<sup>2</sup> we expected r08019 to transiently lose control of SIV replication following infusion of a CD8-depleting mAb. Of interest, the CD8 glycoprotein can be expressed as two isoforms: either as a heterodimer consisting of the CD8 $\alpha$  and CD8 $\beta$  chains (CD8 $\alpha\beta$ ) or as a CD8 $\alpha\alpha$  homodimer.<sup>37</sup> While CD8 $\alpha\beta$  marks thymus-selected MHC class I-restricted T cells,<sup>37,50</sup> CD8 $\alpha\alpha$  is found primarily on mucosal T cells and, in the case of rhesus macaques, NK cells as well.<sup>51,52</sup> Historically, *in vivo* depletion of CD8<sup>+</sup> lymphocytes in SIV-infected rhesus macaques has been accomplished by the infusion of antibodies specific for the CD8 $\alpha$  chain.<sup>5,53,54</sup> An important caveat of this approach is the simultaneous elimination of CD8 $\alpha\beta$ <sup>+</sup> T cells and NK cells, which makes it difficult to distinguish the contribution of each lymphocyte subset to control of SIV infection. To avoid this limitation, we used a newly available rhesus recombinant CDR-grafted mAb (CD8 $\beta$ 255R1) specific for the CD8 $\beta$  chain to selectively ablate CD8 $\alpha\beta$ <sup>+</sup> T cells in r08019 and in both Group 1 macaques (Fig. 3A). Importantly, quality assessment tests performed before the CD8 $\beta$  depletion confirmed that CD8 $\beta$ 255R1 did not block the fluorochrome-labeled anti-CD8 antibodies utilized in our immunophenotyping assays (see Materials and Methods section). A single infusion of 50 mg/kg of CD8 $\beta$ 255R1 readily depleted the majority of

peripheral CD8 $\alpha\beta$ <sup>+</sup> T cells in all three animals without eliminating NK cells (Fig. 3B, C). In fact, NK cell numbers steadily increased following the CD8 $\beta$ 255R1 infusion and peaked at week 9 post CD8 $\beta$  depletion (Fig. 3C). Absolute counts of CD8 $\alpha\alpha$ <sup>+</sup> T cells also rose during this period, especially in r07032 (Fig. 3D). CD4<sup>+</sup> T lymphocyte counts went up as well (Fig. 3E), possibly due to the homeostatic expansion of memory CD4<sup>+</sup> T cells that occurs in response to CD8 depletion *in vivo*.<sup>55</sup> Similar to previous CD8 $\alpha$  depletion studies in SIV-infected elite controller macaques,<sup>2</sup> elimination of CD8 $\alpha\beta$ <sup>+</sup> T cells in the Group 1 animals resulted in a transient increase in viremia (Fig. 3F). While r04132 promptly reasserted control of viral replication, VLs in r07032 remained higher than their baseline levels for several weeks after the CD8 $\beta$  depletion (Fig. 3F). Interestingly, the rise in absolute counts of CD8 $\alpha\alpha$ <sup>+</sup> T cells and NK cells coincided with decreases in viremia in the *Mamu-B\*08*<sup>+</sup> Group 1 macaques (Fig. 3C, D, F), implying that these CD8 $\alpha\alpha$ -expressing lymphocytes contributed to restoring virologic control in those animals. Strikingly, except for borderline VLs (up to 30 vRNA copies/ml) shortly after the CD8 $\beta$  depletion, r08019 did not lose control of SIV replication and had undetectable viremia by week 4.4 post CD8 $\beta$  depletion (Fig. 3F). Small increases in SIV-producing cells in lymph nodes were also observed in r08019 following depletion of its CD8 $\alpha\beta$ <sup>+</sup> T lymphocytes, as determined by *in situ* hybridization performed on biopsies collected before and after the mAb infusion (data not shown). This strange result suggested that an intact CD8 $\alpha\beta$ <sup>+</sup> T cell compartment was not necessary for suppressing SIVmac239 replication in r08019.

To determine if the ability of r08019 to maintain control of viral replication in the context of CD8 $\alpha\beta$ <sup>+</sup> T cell deficiency could be manifested by other macaques with controlled SIV viremia, we subjected two additional animals to the same CD8 $\beta$  depletion regimen described above (Fig. 4). Macaques r09089 and r09037 (Group 3) expressed *Mamu-B\*08*<sup>+</sup> and both controlled SIVmac239 replication as part of a recent experiment conducted by our laboratory (Table 1).<sup>32</sup> As

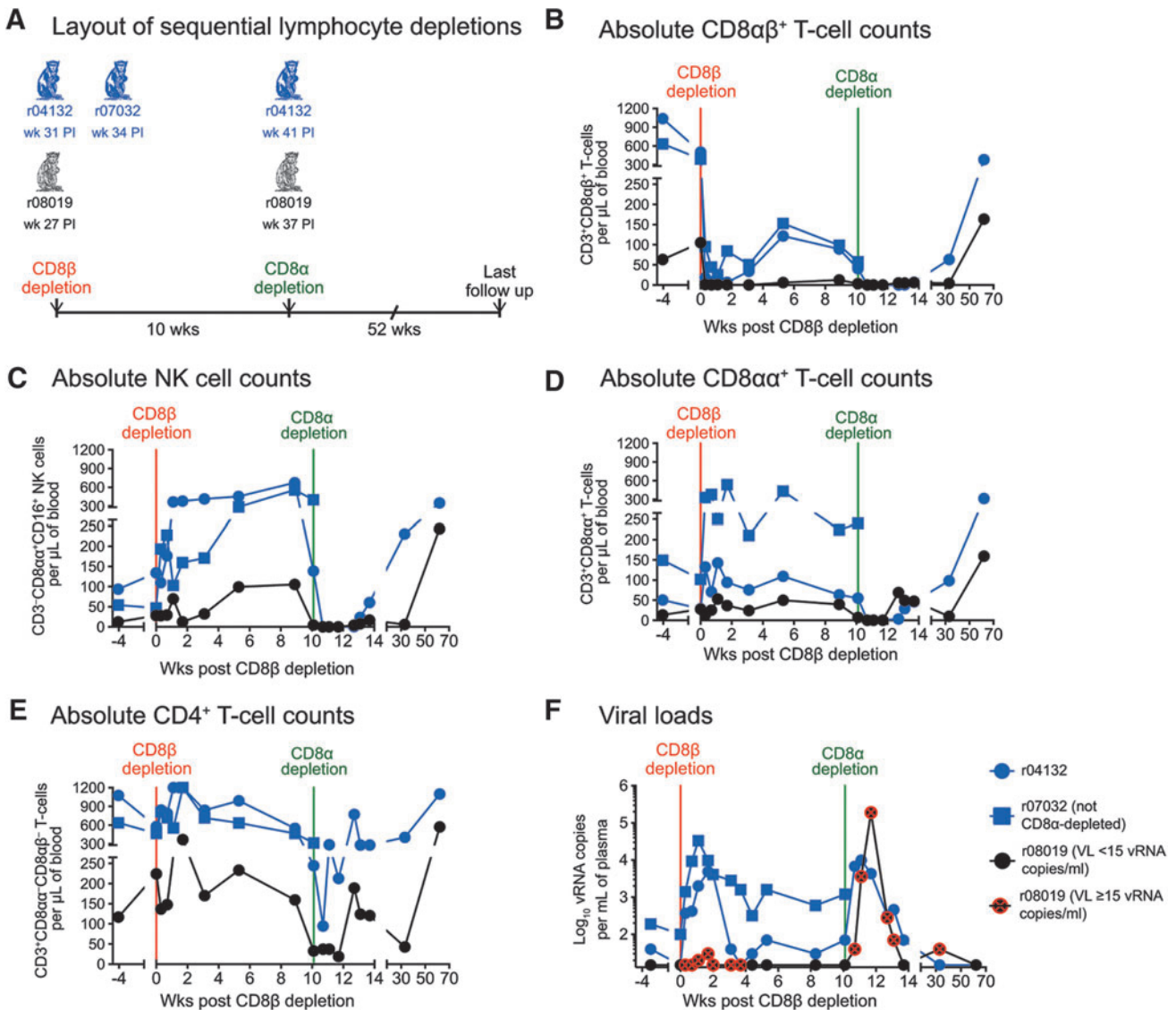


**FIG. 3.** Outcome of sequential *in vivo* lymphocyte depletions. (A) Both Group 1 vaccinees (r04132 and r07032) and r08019 received a single infusion of 50 mg/kg of a new CD8 $\beta$ -specific mAb (CD8 $\beta$ 255R1) designed to deplete CD8 $\beta$ -expressing cells *in vivo*. At the time of the CD8 $\beta$  depletion, r04132 was at week 31 PI; r07032 was at week 34 PI; and r08019 was at week 27 PI. Ten weeks after the CD8 $\beta$  depletion, CD8 $\alpha^+$  lymphocytes in r04132 and r08019 were depleted by a single infusion of 50 mg/kg of the anti-CD8 $\alpha$  mAb MT807R1. Due to adverse events experienced during the CD8 $\beta$  depletion, r07032 was not subjected to this treatment. (B–E) Absolute lymphocyte counts in blood following the CD8 $\beta$  and CD8 $\alpha$  depletions. (B) CD8 $\alpha\beta^+$  T cells (live CD3 $^+$ CD8 $\alpha\alpha^-$ CD8 $\alpha\beta^+$  lymphocytes). (C) NK cells (live CD3 $^+$ CD8 $\alpha\alpha^+$ CD16 $^+$  lymphocytes). (D) CD8 $\alpha\alpha^+$  T cells (live CD3 $^+$ CD8 $\alpha\alpha^+$ CD8 $\alpha\beta^-$  lymphocytes). (E) CD4 $^+$  T cells (considered as live CD3 $^+$ CD8 $\alpha\alpha^-$ CD8 $\alpha\beta^-$  lymphocytes). (F) Log-transformed VLs after the CD8 $\beta$  and CD8 $\alpha$  depletions. The time points when r08019 experienced VLs at or above the limit of reliable quantitation (15 vRNA copies/ml) are crossed in red. VLs in this animal were <15 vRNA copies/ml at all other time points shown in panel (F). mAb, monoclonal antibody.

described above, a single infusion of the CD8 $\beta$ 255R1 mAb resulted in near complete elimination of peripheral CD8 $\alpha\beta^+$  T cells and a rise in NK cell counts in both r09089 and r09037, but especially in the former animal (Fig. 4A, B). Fluctuations in absolute counts of CD4 $^+$  T cells and a modest increase in CD8 $\alpha\alpha^+$  T cell numbers also ensued from the anti-CD8 $\beta$  mAb treatment (Fig. 4D, E). In contrast to r08019, but similar to the Group 1 macaques, both Group 3 macaques experienced a surge in viremia after depletion of their CD8 $\alpha\beta^+$  T cells (Fig. 4F). Although r09037 transiently regained control of viral replication at week 4 posttreatment, SIV rebounded

again shortly thereafter and VLs eventually leveled off at 100–1,000 vRNA copies/ml (Fig. 4F). Monkey r09089 never reasserted full control of viral replication and its VLs ultimately plateaued in the same range as that of r09037 (Fig. 4F). These results indicated that the lack of SIV rebound manifested by r08019 in the context of CD8 $\alpha\beta^+$  T cell deficiency was not a general feature of controlled SIV infection.

Next, we set out to explore whether CD8 $\alpha\alpha$ -expressing cells prevented SIV rebound in r08019 when its CD8 $\alpha\beta^+$  T cells were eliminated. To address this possibility, we planned to treat r08019 and r04132 with the mouse/rhesus CDR-



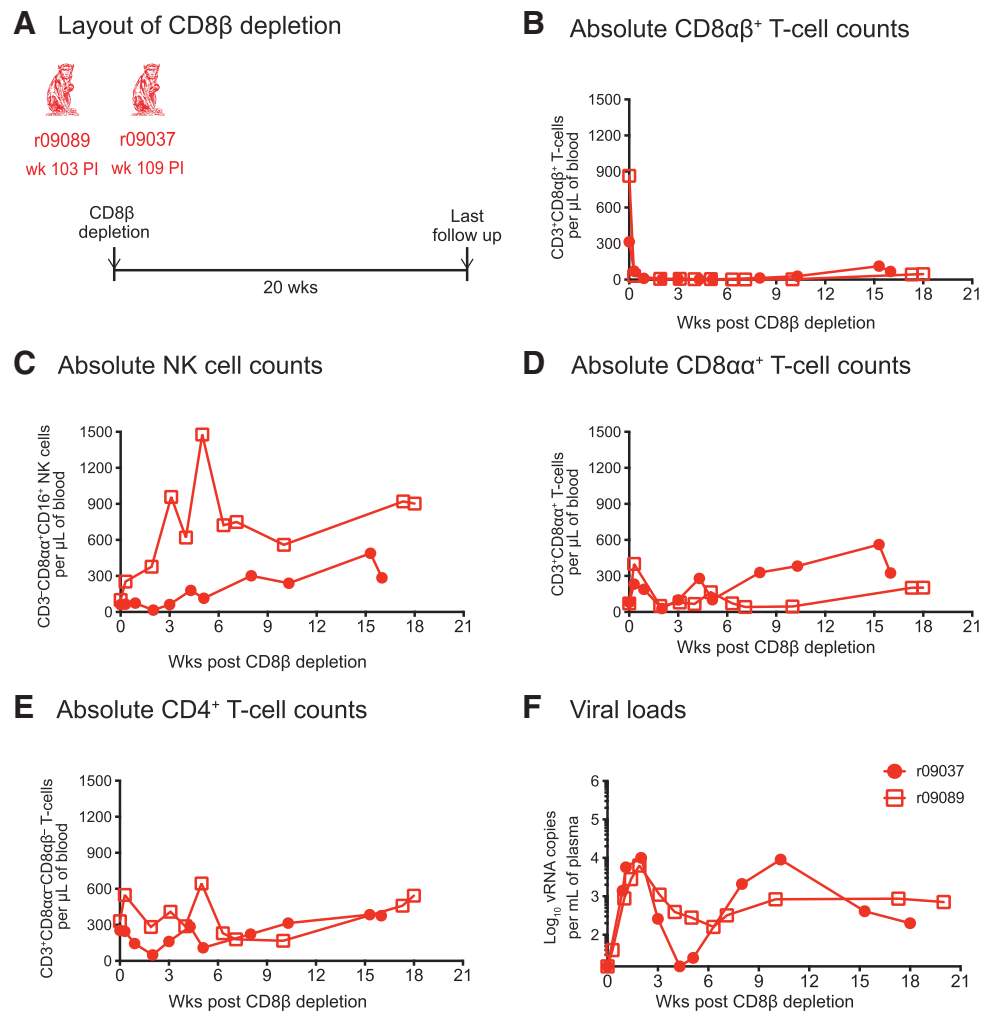


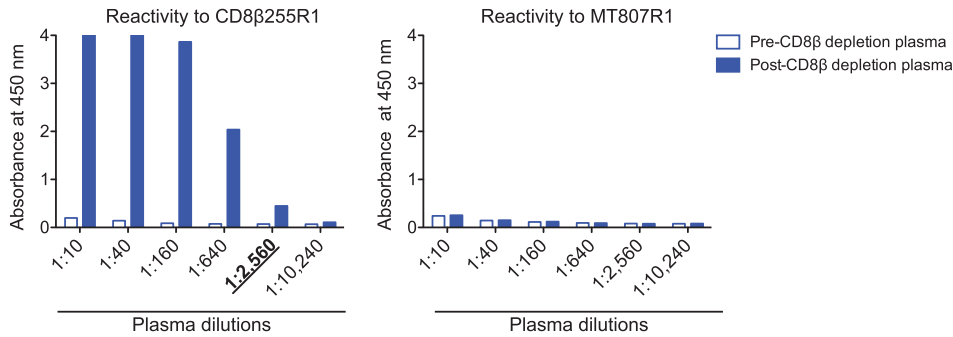
**FIG. 4.** Outcome of CD8 $\beta$  depletion in two additional SIV-infected macaques manifesting control of chronic phase viremia. **(A)** The *Mamu-B\*08*<sup>+</sup> rhesus macaques r09089 and r09037 were rectally infected with SIV<sub>mac239</sub> as part of a recent experiment conducted by our laboratory and controlled chronic phase viremia.<sup>32</sup> Similar to the procedure described in Figure 3, these animals received a single infusion of 50 mg/kg of the CD8 $\beta$ 255R1 mAb. At the time of the CD8 $\beta$  depletion, r09089 was at week 103 PI and r09037 was at week 109 PI. **(B–E)** Absolute lymphocyte counts in blood following the CD8 $\beta$  and CD8 $\alpha$  depletions. **(B)** CD8 $\alpha\beta^+$  T cells (live CD3<sup>+</sup>CD8 $\alpha\alpha^-$ CD8 $\alpha\beta^+$  lymphocytes). **(C)** NK cells (live CD3<sup>+</sup>CD8 $\alpha\alpha^+$ CD16<sup>+</sup> lymphocytes). **(D)** CD8 $\alpha\alpha^+$  T cells (live CD3<sup>+</sup>CD8 $\alpha\alpha^+$ CD8 $\alpha\beta^-$  lymphocytes). **(E)** CD4 $^+$  T cells (considered as live CD3<sup>+</sup>CD8 $\alpha\alpha^-$ CD8 $\alpha\beta^-$  lymphocytes). **(F)** Log-transformed VLs after the CD8 $\beta$  depletion.

grafted anti-CD8 $\alpha$  mAb MT807R1 at week 10 post CD8 $\beta$  depletion. We decided not to subject r07032 to this procedure since this animal had experienced adverse events during the CD8 $\beta$ 255R1 infusion. A potential risk of this experiment was the development of anaphylactic reactions triggered by anti-CD8 $\beta$ 255R1 antibodies reacting against the MT807R1 Ig molecule. To estimate the levels of these cross-reactive anti-Ig responses, we coated ELISA plates with either CD8 $\beta$ 255R1 or MT807R1 and screened pre- and post-CD8 $\beta$  depletion plasma for the presence of anti-Ig antibodies. The goal of this assay was to determine the highest plasma dilution where the OD value of the postdepletion sample was >2-fold higher than the corresponding predepletion sample (i.e., the end point titer). As expected, both r04132 and r08019 developed anti-CD8 $\beta$ 255R1 antibodies after the CD8 $\beta$  depletion, with end point titers of 2,560 and 160, respectively (Fig. 5). However, we could not determine the end point titer of cross-reactive anti-MT807R1 antibodies in these monkeys since their pre-

and post-CD8 $\beta$  depletion plasma samples yielded largely equivalent OD values, even at the lowest dilution (1:10) tested (Fig. 5). Since these data suggested that r08019 and r04132 had little or no anti-MT807R1 antibodies, we decided to proceed with the CD8 $\alpha$  depletion.

Even though we could not detect anti-MT807R1 antibodies in r08019, this animal experienced decreased oxygen saturation, abnormal heart rates, and vomiting during the MT807R1 infusion. Monkey r08019 recovered after receiving supportive care, but ended up being treated with half of the planned dose of MT807R1. Conversely, r04132 did not experience any adverse reactions and received the full dose of MT807R1. Although we administered only half of the desired amount of the anti-CD8 $\alpha$  mAb to r08019, this dose was sufficient to transiently eliminate peripheral CD8 $\alpha$ -expressing (CD8 $\alpha\alpha^+$  and CD8 $\alpha\beta^+$ ) T lymphocytes and NK cells in this animal (Fig. 3B–D). Strikingly, SIV swiftly rebounded in r08019, peaking at 190,000 vRNA copies/ml on day 11 post CD8 $\alpha$  depletion

### A Endpoint titers of anti-Ig antibodies in r04132



### B Endpoint titers of anti-Ig antibodies in r08019

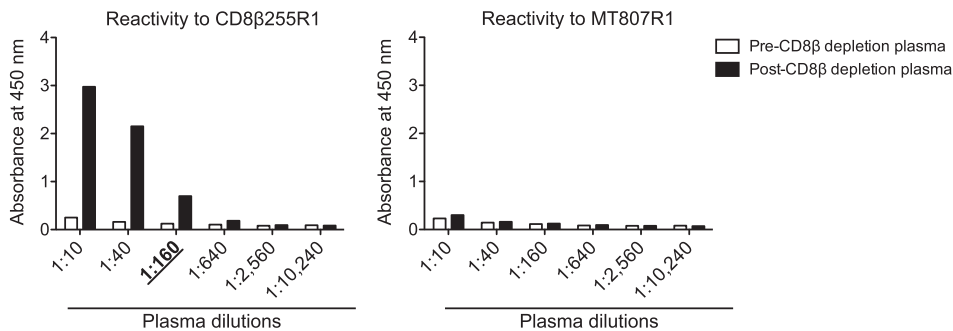


**FIG. 5.** End point titers of anti-Ig antibodies in r04132 and r08019. Pre- and post-CD8 $\beta$  depletion plasma from r04132 (**A**) and r08019 (**B**) was tested for reactivity to the CD8 $\beta$ 255R1 (*left panels*) and MT807R1 (*right panels*) mAbs. The goal of this assay was to determine the end point titer of antibodies against each mAb, that is, the highest plasma dilution where the absorbance level of the postdepletion sample was >2-fold higher than the corresponding predepletion sample. Plasma saved 8 days before and 22 days after the CD8 $\beta$ 255R1 infusion served as the pre- and postdepletion samples, respectively. The end point titers of anti-CD8 $\beta$ 255R1 antibodies are *underlined* and in *boldface* type below each graph. Anti-MT807R1 antibodies could not be detected in either r04132 or r08019 by this methodology. Ig, immunoglobulin.

(week 38.4 PI; Fig. 3F). Macaque r04132 also experienced a brief rise in viremia that peaked at 9,900 vRNA copies/ml (Fig. 3F). Both animals regained control of viral replication in the ensuing weeks, concomitant with increases in absolute numbers of peripheral CD8 $\alpha\alpha^+$  T cells and NK cells (Fig. 3C, D, F). CD4 $^+$  T lymphocytes also expanded during this period, likely as a result of the CD8 $\alpha$  depletion (Fig. 3E). These data suggested that effector lymphocytes expressing CD8 $\alpha\alpha$  homodimers, but not CD8 $\alpha\beta$  heterodimers, were responsible for maintaining virologic control in r08019.

Infection with replication-impaired lentiviruses can also lead to controlled viremia, as evidenced by the detection of defective HIV-1 variants in long-term nonprogressor patients.<sup>56–61</sup> To address this possibility, we set out to determine if the virus that infected r08019 harbored any unusual insertions, deletions, or mutations. We first searched for genetic variation in proviral sequences amplified from cryopreserved PBMC collected at week 2 PI (Fig. 6A). All proviral sequences identified by this analysis contained two amino acid substitutions in Env (C<sub>432</sub>W and I<sub>863</sub>M; data not shown) and one in Nef (Y<sub>39</sub>C; Fig. 6B). In addition, an 18-bp in-frame deletion in *nef* corresponding to aa<sub>139</sub>HRILDI<sub>144</sub> was present in 100% of the sequence reads (Fig. 6B, C). Interestingly, a similar 12-bp *nef* deletion affecting aa<sub>143</sub>DIYL<sub>146</sub> is found in the SIVmacC8 clone (Fig. 6B), which has been widely used as a live-attenuated SIV vaccine.<sup>62–66</sup> The highly conserved core region of Nef altered by this deletion is functionally constrained, as evidenced by the instability and functionally impaired activity of the SIVmacC8 Nef protein.<sup>67</sup> Moreover, SIVmac239 Nef lacking the same four amino acids that are absent from the SIVmacC8 Nef protein also exhibits the same dysfunctional phenotype.<sup>67</sup> Based on the similarity between the SIVmacC8

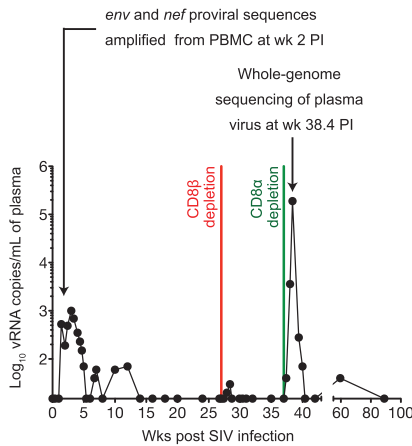
*nef* deletion and the deletion found in the virus discovered in r08019, we concluded that this animal harbored an attenuated SIV variant as early as week 2 PI.

Curiously, the six amino acids affected by this deletion are contained within the Mamu-B\*08-restricted Nef<sub>137–146</sub>RL10 epitope. Despite this coincidence, r08019 tested negative for Mamu-B\*08 in two independent MHC typing assays. Moreover, r08019 did not have detectable Nef-specific T cell responses in an ICS assay performed at week 3.4 PI (Fig. 7), consistent with a mechanism for the emergence of the *nef* deletion that was independent from viral escape driven by T cell pressure.

To rule out the possibility that the *nef* deletion detected in r08019 was an experimental artifact, we sequenced the virus that rebounded following the CD8 $\alpha$  depletion. Strikingly, 100% of circulating viral quasiespecies contained the same deletion affecting aa<sub>139</sub>HRILDI<sub>144</sub> at week 38.4 PI, the peak of rebound viremia (Fig. 6A, B). These viruses also exhibited signs of CD8 $^+$  T cell-driven sequence evolution, as shown by escape mutations in the Mamu-A\*01-restricted Tat<sub>28–35</sub>SL8 and Env<sub>726–735</sub>ST10 epitopes (data not shown).<sup>68</sup> However, the Gag<sub>181–189</sub>CM9 epitope was intact at this time point (data not shown). Of note, the Env (C<sub>432</sub>W and I<sub>863</sub>M) and Nef (Y<sub>39</sub>C) substitutions detected in cell-associated DNA at week 2 PI were absent from plasma vRNA, indicating possible reversions (data not shown; Fig. 6B). These data confirmed our previous sequencing results and showed that the *nef* deletion was stably maintained in the course of r08019's infection.

Finally, we investigated the origin of the *nef* deletion detected in r08019. Since this polymorphism was already present at week 2 PI, we explored whether the challenge inoculum contained *nef*-deleted SIV variants that could have initiated

**A** Scheme of viral sequencing analysis in monkey r08019



**B** Alignment of predicted Nef amino acid sequences found in r08019

PBMC SIV DNA wk 2 PI	MGGAI SMRRSRPSGDLRQRLLRARGETYGRLLGEVEDG	QSPGGLDKGLSSLSCEGQKY	60
Plasma SIV RNA wk 38.4 PI	MGGAI SMRRSRPSGDLRQRLLRARGETYGRLLGEVEDG	QSPGGLDKGLSSLSCEGQKY	60
SIVmac239	*****	*****	60
PBMC SIV DNA wk 2 PI	NQGQYMNTPWRNPAEEREKLAYRKQNMDDIDEEDDDLVGVSVRPKVPLRTMSYKLAIDMS		120
Plasma SIV RNA wk 38.4 PI	NQGQYMNTPWRNPAEEREKLAYRKQNMDDIDEEDDDLVGVSVRPKVPLRTMSYKLAIDMS		120
SIVmac239	*****	*****	120
PBMC SIV DNA wk 2 PI	HFIEKGGLEGIIYSARR	YLEKEEGLIPDQDYTSGPGIRYKPTFGWLKLVVP	174
Plasma SIV RNA wk 38.4 PI	HFIEKGGLEGIIYSARR	YLEKEEGLIPDQDYTSGPGIRYKPTFGWLKLVVP	174
SIVmac239	*****	*****	180
PBMC SIV DNA wk 2 PI	NVSDAQDEDEHYLMHPAQTQWDDPWGEVLAWKFDPTLAYTYEAYVRYPEEFGSKSGLS		234
Plasma SIV RNA wk 38.4 PI	NVSDAQDEDEHYLMHPAQTQWDDPWGEVLAWKFDPTLAYTYEAYVRYPEEFGSKSGLS		234
SIVmac239	*****	*****	240
PBMC SIV DNA wk 2 PI	EEVRRRLTARGLLNMADKKETR		257
Plasma SIV RNA wk 38.4 PI	EEVRRRLTARGLLNMADKKETR		257
SIVmac239	EEVRRRLTARGLLNMADKKETR		263

\* Fully conserved residues

**C** Short nucleotide direct repeats near the ends of the nef deletion

9,490      9,500      9,510      9,520

gcaagaagacatagaatcttagacatatacttagaaaag

A R R H R I L D I Y L E K

Deletion of aa 139-144

**FIG. 6.** Viral sequencing analysis in r08019. **(A)** Scheme of the viral sequencing analysis performed in r08019. We searched for genetic variation in SIV DNA obtained from cryopreserved PBMC collected at week 2 PI. Viral sequences from nucleotides 7,565–9,979 were amplified, which encode aa 324–879 of Env and the entire Nef protein (aa 1–263). Eleven days after the infection of the anti-CD8 $\alpha$  mAb, when r08019 experienced a VL of 190,000 vRNA copies/ml (week 38.4 PI), we isolated vRNA from plasma and sequenced the SIV genomes circulating at this time point. **(B)** Alignment of predicted Nef amino acid sequences found in r08019. Conceptual translations of the nef sequences obtained from PBMC-associated SIV DNA at week 2 PI and from plasma vRNA at week 38.4 PI are shown in the upper rows. As a reference, the aa sequence of the SIVmac239 Nef protein is shown in the bottom row. The location of the six-amino acid Nef deletion (139HRILDI144) found in r08019 is indicated by a box. The Y39C substitution present in SIV DNA at week 2 PI is also enclosed by a box. However, this mutation was not detected in the rebounding virus following the CD8 $\alpha$  depletion. The sequence corresponding to the SIVmacC8 nef deletion is underlined. **(C)** Short direct nucleotide repeats near the limits of the deleted region in nef are underlined. These repeated stretches are 8 nucleotides long, seven of which are identical in each repeat. The position of the nucleotides relative to the SIVmac239 genome is indicated on top, and the deleted aa region is enclosed by a box. The nef deletion overlaps with the 3' long terminal repeat U3 region, which spans nucleotides 9,452–9,978.

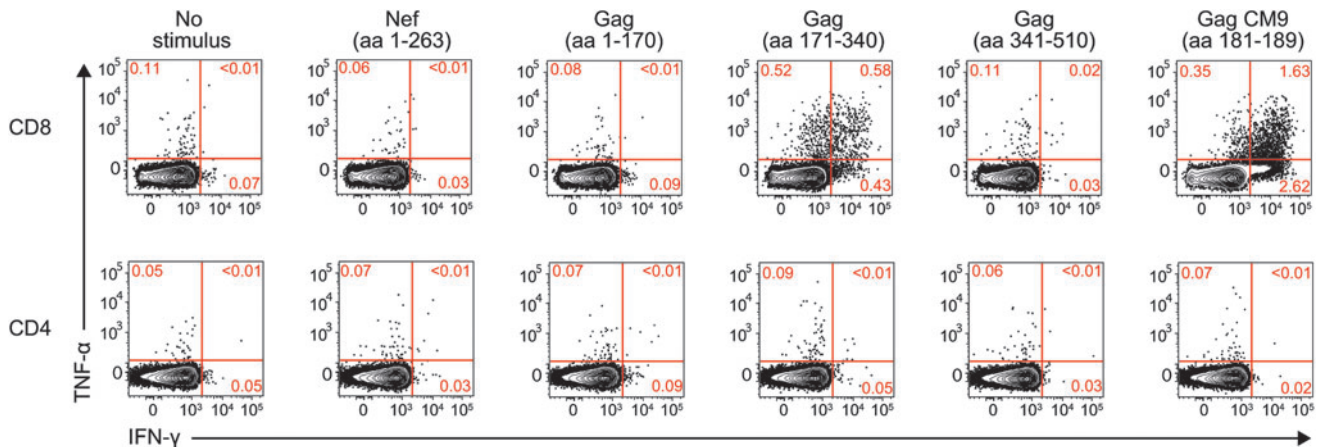


**FIG. 7.** Postinfection analysis of SIV-specific T cell responses in r08019. We carried out an intracellular cytokine staining assay in PBMC from r08019 at week 3.4 PI. The stimuli consisted of pools of peptides spanning the entire Nef protein or three segments of the Gag polyprotein. A peptide corresponding to the Mamu-A\*01-restricted Gag<sub>181–189</sub>CM9 epitope was included as well. Reactivity to each stimulus is shown based on the production of IFN- $\gamma$  and/or TNF- $\alpha$ . CD8<sup>+</sup> and CD4<sup>+</sup> T lymphocytes are shown in the top and bottom rows, respectively.

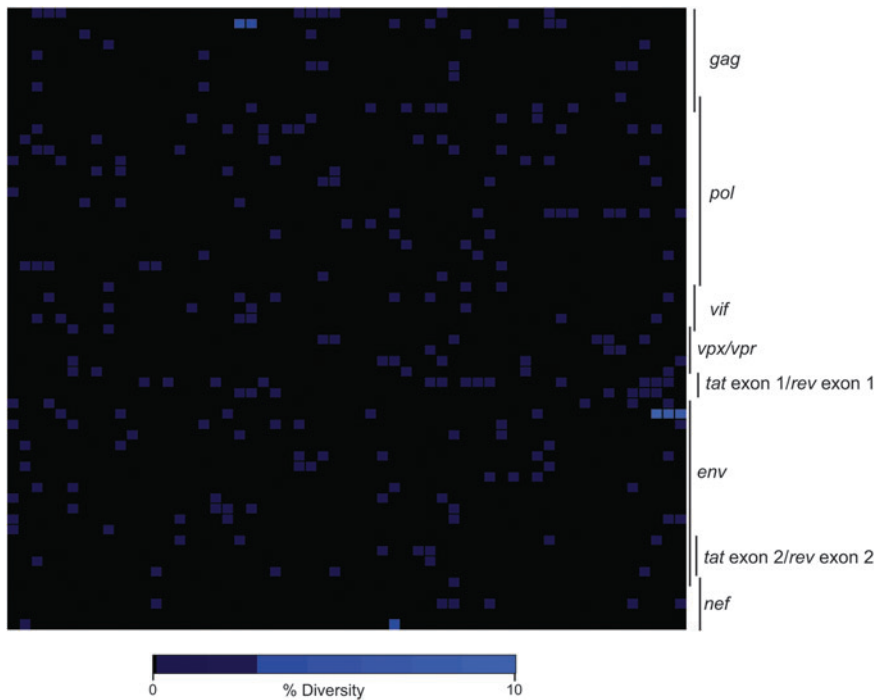


**FIG. 8.** Genome-wide deep sequencing of the SIVmac239 stock used for the IR challenges. Heat map illustration of the level of sequence variation across the SIVmac239 genome detected from 454 deep sequencing. Plotted is the percentage of amino acid diversity at each position across the genome with the first amino acid of Gag located in the *top left* corner of the grid and the last amino acid of Nef located in the *bottom right* corner. Completely conserved codons are *black*, and low-level variant residues (<10%) are colored *light blue*.

infection in r08019. To do that, we performed whole genome sequencing on our SIVmac239 challenge stock, which was produced by propagating the supernatant from transfected 293T cells on PBMC from SIV naive rhesus macaques over several days. This analysis revealed a relatively homogeneous virus population, with low levels of viral diversity detected across the genome (Fig. 8). Importantly, there was no evidence of the *nef* deletion in the stock, although the aforementioned Env (C<sub>432</sub>W and I<sub>863</sub>M) and Nef (Y<sub>39</sub>C) amino acid substitutions were present at extremely low frequencies (<0.05%). Of note, the threshold frequency for detecting mutant species in this analysis was 0.05%, considering that each sequencing reaction contained ~2,000 copies of viral template. These results implied that either the *nef* deletion arose *in vivo* shortly after r08019 became infected or that a rare SIV variant bearing this polymorphism was present in the challenge inoculum, which went undetected by our sequencing approach, and somehow managed to infect r08019.

## Discussion

In this study, we report the efficacy of a rDNA/rYF17D/rRRV PBB regimen encoding immunodominant SIV epitopes against repeated IR challenges with SIVmac239. Both *Mamu-B\*08*<sup>+</sup> Group 1 vaccinees controlled viral replication to levels rarely seen among MHC class I-matched historical control macaques that have been previously infected with SIVmac239. CD8 $\alpha\beta$ <sup>+</sup> T lymphocytes were likely responsible for this impressive outcome as mAb-mediated depletion of these cells resulted in transient increases in viremia. As for the *Mamu-A\*01*<sup>+</sup> Group 2 vaccinee r08019, virologic control appeared to involve CD8 $\alpha\beta$ <sup>+</sup> lymphocytes and an attenuating deletion in the *nef* gene, although it is also possible that SIV-specific CD8 $\alpha\beta$ <sup>+</sup> T cells participated in viral containment before the CD8 $\beta$  depletion. Although the mechanism underlying r08019's impressive containment of SIV infection

might not be generalizable, the uniqueness of this animal's course of infection illustrates the complexity of lentivirus-host interactions.

The discovery of a *nef*-deleted SIV variant in r08019 remains a puzzling aspect of this study since this virus was found in all proviral sequences amplified at week 2 PI, but not in the challenge inoculum. Assuming that the low dose SIVmac239 IR challenge regimen used in this study resulted in the transmission of a single virus, we can envision at least three possible explanations for the origin of this *nef*-deleted mutant. First, despite our inability to detect this deleted form in the SIVmac239 challenge stock, we cannot rigorously rule out the possibility that a minor variant harboring this change is what was transmitted. Indeed, deep sequencing of the inoculum revealed low levels of sequence diversity, probably as a result of propagating the virus on mitogen-activated rhesus macaque PBMC as part of its derivation method.<sup>69</sup> Given the error-prone nature of retroviral reverse transcription, the low frequency SIV variants detected in the stock likely represent byproducts of multiple rounds of viral replication *in vitro*. Furthermore, our inability to detect the *nef*-deleted virus in this stock would be in keeping with the technical problems inherent in searching for a rare polymorphism in a highly concentrated sample made almost exclusively of WT genomes.

Second, it is also possible that a reverse transcription error occurred in the first round of viral replication *in vivo*, resulting in the *nef* deletion in question. Indeed, short direct repeats are present near the ends of the 18-bp deletion in the SIVmac239 clone (Fig. 6C), similar to what has been observed in other examples of appearance of deletions in *nef*.<sup>70</sup> These short direct repeats have been associated with the emergence of deletions in retroviral genomes by a mechanism involving template slippage during the reverse transcriptase reaction.<sup>71,72</sup>

A third possibility is that the *nef* deletion was selected for *in vivo* within the first 2 weeks after r08019 became infected.



Although this 2-week time frame might appear too short for the selection of the *nef*-deleted mutant, there is precedent for immunological pressures resulting in an altered variant virus with similar kinetics.<sup>32,58,73</sup> While the nature of the selection event(s) implicit in this model remains unknown, it probably did not involve T cell responses since r08019 had no detectable Nef-specific T cells in the acute phase (Fig. 7). Alternatively, the *nef* deletion might have emerged in response to selective pressure imposed by NK cells, potentially by a mechanism involving killer immunoglobulin-like receptor (KIR) recognition of viral epitopes presented by MHC class I molecules.<sup>74</sup> Along these lines, specific aa substitutions in the HIV-1 proteome have been reported to be significantly enriched in infected individuals expressing combinations of KIR and MHC class I alleles, indicating that NK cells can drive HIV-1 escape.<sup>75,76</sup> Given the high epitope density of the core region of Nef,<sup>77</sup> the deleted virus found in r08019 may have been selected for by KIR-expressing NK cells targeting a peptide in that region. Much more extensive analysis will be required to investigate this last possibility.

The use of a new anti-CD8 $\beta$  mAb that selectively eliminates CD8 $\alpha\beta^+$  T lymphocytes *in vivo* without the caveat of depleting CD8 $\alpha\alpha$ -expressing rhesus macaque NK cells was a key part of this study. A single infusion of this antibody resulted in a surge of SIV replication in the Group 1 macaques but, surprisingly, not in r08019, indicating that this animal did not require an intact CD8 $\alpha\beta^+$  T cell compartment to maintain control of chronic phase viremia. Importantly, the *nef*-deleted SIV variant that infected r08019 was clearly replication competent, as evidenced by the sharp rise in VL triggered by the subsequent CD8 $\alpha$  depletion. These findings are intriguing and raise the question of what prevented this variant from rebounding in r08019 after the CD8 $\beta$  depletion. Of note, mAb-directed elimination of lymphocytes in tissues can be less efficient than what is observed in blood. Indeed, macaques subjected to the same CD8 $\beta$ 255R1 infusion utilized in this study exhibited incomplete depletion of CD8 $^+$  T cells in lymph node and duodenal biopsies in the first few weeks after the CD8 $\beta$ 255R1 infusion ([www.nhpreagents.org/NHP/Download.aspx?View=1&FileGUID=b7154cabe30-431c-834a-444c9376](http://www.nhpreagents.org/NHP/Download.aspx?View=1&FileGUID=b7154cabe30-431c-834a-444c9376)). In this regard, we cannot discard the possibility that residual SIV-specific CD8 $\alpha\beta^+$  T cells present in relevant sites of SIV persistence prevented virus rebound in r08019 following the CD8 $\beta$ 255R1 infusion. Alternatively, NK cells could also have suppressed viral replication during the period of CD8 $\alpha\beta^+$  T cell deficiency. Along these lines, a vigorous expansion of NK cells coincided with the reestablishment of virologic control in the Group 1 macaques. Although epidemiological and *in vitro* data support a role for NK cells in lentivirus control,<sup>78</sup> previous attempts to deplete these lymphocytes *in vivo* by the infusion of an anti-CD16 mAb revealed no significant contribution to the containment of SIV infection.<sup>79,80</sup> Critically, however, the majority of rhesus macaque NK cells in the gut and vaginal mucosae do not express CD16,<sup>81</sup> indicating that *in vivo* depletion of CD16 $^+$  cells might not address the antiviral potential of tissue-resident NK cells. Considering this heterogeneity, it is difficult to assess the extent to which NK cells controlled viral replication in r08019 since our phenotypic analysis focused on CD3 $^-$ CD8 $\alpha\alpha^+$ CD16 $^+$  cells—the dominant NK cell subset in macaque peripheral blood.<sup>52</sup> Thus, while our data provide circumstantial evidence for NK

cell-mediated control of SIV replication in one animal, they also illustrate the challenges of studying NK cells in non-human primates without more inclusive and selective strategies for depleting these lymphocytes *in vivo*.

Given the increase in CD8 $\alpha\alpha^+$  T cell counts after the CD8 $\beta$  depletion, especially in the Group 1 macaque r07032, we also considered the possibility that these cells contributed to control of SIV replication during this period. The physiological role of CD8 $\alpha\alpha$  homodimers expressed by T cells is not completely understood. Previous studies in mice have shown that while both CD8 $\alpha\alpha$  and CD8 $\alpha\beta$  isoforms can bind to MHC class I molecules,<sup>82–84</sup> CD8 $\alpha\beta$  heterodimers appear to be required for the selection of MHC class I-restricted CD8 $^+$  T lymphocytes in the thymus.<sup>50</sup> Furthermore, the CD8 $\alpha\alpha$  molecule has been described as a marker for T cell activation and is primarily expressed by mucosal T cells.<sup>51,85,86</sup> Interestingly, human CD8 $\alpha\alpha^+$  T cells residing in genital skin have been recently implicated in the containment of herpes simplex virus-2 reactivation,<sup>87</sup> indicating that these cells participate in defense against persistent viral infections. Although CD8 $\alpha\alpha^+$  T cells might be part of a unique, regionally specialized, lineage of T lymphocytes, it is not clear if the peripheral CD8 $\alpha\alpha^+$  T cells identified in this study are examples of such cells. Alternatively, they could have comprised preexisting CD8 $\alpha\alpha^+$ CD8 $\alpha\beta^+$  T cells in PBMC that internalized their surface CD8 $\alpha\beta$  heterodimers upon ligation of the anti-CD8 $\beta$  mAb. A detailed analysis of the T cell receptor clonotypes, Ag specificities, and tissue distribution of CD8 $\alpha\alpha^+$  and CD8 $\alpha\beta^+$  T cells before and after depletion of CD8 $\alpha\beta^+$  lymphocytes would have been needed to address this possibility. Nevertheless, in light of the recent identification of tissue-resident human CD8 $\alpha\alpha^+$  T cells endowed with potent antiviral activity,<sup>87</sup> characterizing the role of these unconventional T lymphocytes during lentivirus infections may lead to new strategies for eliciting cellular immunity against HIV.

In conclusion, in this study we show that SIV-specific CD8 $^+$  T cells elicited by a rDNA/rYF17D/rRRV PBB regimen afforded significant control of SIV<sub>mac239</sub> replication in 3/4 vaccinees. Since vaccine-induced CD8 $^+$  T cells in these animals were focused on a single immunodominant SIV epitope, we are currently exploring if expanding the CD8 $^+$  T cell response against other viral Ags can improve vaccine efficacy. We also explored the basis for the unusual control of SIV<sub>mac239</sub> replication manifested by one vaccinated macaque and showed that, surprisingly, this animal harbored a *nef*-deleted mutant as early as 2 weeks PI. Subsequent CD8 depletions suggested that replication of this SIV variant may have been contained by CD8 $\alpha\alpha$ -expressing lymphocytes, warranting further investigation of the antiviral capacity of NK cells *in vivo*. While we could not pinpoint the origin of the *nef*-deleted virus, three possible explanations involving both stochastic and selective events were presented based on the available data. Collectively, these data provide additional insights into the full spectrum of virologic control of lentivirus infection.

#### Acknowledgments

The authors are grateful to Brandon Keele for helpful comments on this article and to Dr. Elizabeth Connick for quantifying SIV-producing cells in lymph node biopsies by *in situ* hybridization. The authors also thank Rebecca



Shoemaker, Nicholas Pomplun, Jessica Furlott, Randy Fast, Kelli Oswald, Marlon Veloso de Santana, and William Lauer for technical support. The authors also wish to acknowledge Eric Peterson, Kristin Crosno, and Kevin Brunner for providing excellent care of the rhesus macaques used in this experiment; Teresa Maidana Giret for confirming the MHC class I genotype of the monkeys in this study; Leydi Guzman for administrative assistance; and Christopher Parks for facilitating the electroporated rDNA vaccinations used in this study. This work was funded by Public Health Service grant R37AI052056 to D.I.W. and was supported, in part, by federal funds from the National Cancer Institute, National Institutes of Health, under contract no. HHSN261200800001E and from the National Institute of Allergy and Infectious Diseases through P01 AI074415 (T.M.A.). The funders had no role in study design, data collection, and interpretation or the decision to submit the work for publication. The mAbs used in the *in vivo* lymphocyte depletions were produced by the NIH Nonhuman Primate Reagent Resource (OD010976 and HHSN2722001300031C, K.A.R.).

### Disclaimer

TA's spouse was an employee of Bristol-Myers Squibb, which has a focus in Virology, specifically treatments for hepatitis B and C and HIV/AIDS. TA's spouse no longer works for BMS and only retained a small stock interest in the public company. TA's interests were reviewed and managed by Massachusetts General Hospital and Partners HealthCare in accordance with their conflict of interest policies.

### Sequence Data

All reads have been deposited to the NCBI Sequence Read Archive under accession number SRP016012.

### Author Disclosure Statement

No competing financial interests exist.

### References

- Allen TM, Altfeld M, Geer SC, *et al.*: Selective escape from CD8+ T-cell responses represents a major driving force of human immunodeficiency virus type 1 (HIV-1) sequence diversity and reveals constraints on HIV-1 evolution. *J Virol* 2005;79:13239–13249.
- Friedrich TC, Valentine LE, Yant LJ, *et al.*: Subdominant CD8+ T-cell responses are involved in durable control of AIDS virus replication. *J Virol* 2007;81:3465–3476.
- Kiepiela P, Ngumbela K, Thobakgale C, *et al.*: CD8+ T-cell responses to different HIV proteins have discordant associations with viral load. *Nat Med* 2007;13:46–53.
- Koup RA, Safrit JT, Cao Y, *et al.*: Temporal association of cellular immune responses with the initial control of viremia in primary human immunodeficiency virus type 1 syndrome. *J Virol* 1994;68:4650–4655.
- Schmitz JE, Kuroda MJ, Santra S, *et al.*: Control of viremia in simian immunodeficiency virus infection by CD8+ lymphocytes. *Science* 1999;283:857–860.
- Buchbinder SP, Mehrotra DV, Duerr A, *et al.*: Efficacy assessment of a cell-mediated immunity HIV-1 vaccine (the Step Study): A double-blind, randomised, placebo-controlled, test-of-concept trial. *Lancet* 2008;372:1881–1893.
- Gray GE, Allen M, Moodie Z, *et al.*: Safety and efficacy of the HVTN 503/Phambili study of a clade-B-based HIV-1 vaccine in South Africa: A double-blind, randomised, placebo-controlled test-of-concept phase 2b study. *Lancet Infect Dis* 2011;11:507–515.
- Hammer SM, Sobieszczyk ME, Janes H, *et al.*: Efficacy trial of a DNA/rAd5 HIV-1 preventive vaccine. *N Engl J Med* 2013;369:2083–2092.
- Daniel MD, Kirchhoff F, Czajak SC, Sehgal PK, Desrosiers RC: Protective effects of a live attenuated SIV vaccine with a deletion in the nef gene. *Science* 1992;258:1938–1941.
- Fukazawa Y, Park H, Cameron MJ, *et al.*: Lymph node T cell responses predict the efficacy of live attenuated SIV vaccines. *Nat Med* 2012;18:1673–1681.
- Barouch DH: Novel adenovirus vector-based vaccines for HIV-1. *Curr Opin HIV AIDS* 2010;5:386–390.
- Excler JL, Parks CL, Ackland J, Rees H, Gust ID, Koff WC: Replicating viral vectors as HIV vaccines: Summary report from the IAVI-sponsored satellite symposium at the AIDS vaccine 2009 conference. *Biologicals* 2010;38:511–521.
- Pantaleo G, Esteban M, Jacobs B, Tartaglia J: Poxvirus vector-based HIV vaccines. *Curr Opin HIV AIDS* 2010;5:391–396.
- Sardesai NY, Weiner DB: Electroporation delivery of DNA vaccines: Prospects for success. *Curr Opin Immunol* 2011;23:421–429.
- Casimiro DR, Wang F, Schleif WA, *et al.*: Attenuation of simian immunodeficiency virus SIVmac239 infection by prophylactic immunization with dna and recombinant adenoviral vaccine vectors expressing Gag. *J Virol* 2005;79:15547–15555.
- Hel Z, Nacsa J, Tryniszewska E, *et al.*: Containment of simian immunodeficiency virus infection in vaccinated macaques: Correlation with the magnitude of virus-specific pre- and postchallenge CD4+ and CD8+ T cell responses. *J Immunol* 2002;169:4778–4787.
- Hel Z, Tsai WP, Tryniszewska E, *et al.*: Improved vaccine protection from simian AIDS by the addition of nonstructural simian immunodeficiency virus genes. *J Immunol* 2006;176:85–96.
- Lasaro MO, Haut LH, Zhou X, *et al.*: Vaccine-induced T cells provide partial protection against high-dose rectal SIVmac239 challenge of rhesus macaques. *Mol Ther* 2011;19:417–426.
- Liu J, O'Brien KL, Lynch DM, *et al.*: Immune control of an SIV challenge by a T-cell-based vaccine in rhesus monkeys. *Nature* 2009;457:87–91.
- Pellett PE, Roizman B: Herpesviridae. In: *Fields Virology* (Knipe DM, Howley PM, eds.) Lippincott Williams & Wilkins, Philadelphia, PA, 2013, pp. 1802–1819.
- Torti N, Oxenius A: T cell memory in the context of persistent herpes viral infections. *Viruses* 2012;4:1116–1143.
- Masopust D, Schenkel JM: The integration of T cell migration, differentiation and function. *Nat Rev Immunol* 2013;13:309–320.
- Hansen SG, Vieville C, Whizin N, *et al.*: Effector memory T cell responses are associated with protection of rhesus monkeys from mucosal simian immunodeficiency virus challenge. *Nat Med* 2009;15:293–299.
- Hansen SG, Ford JC, Lewis MS, *et al.*: Profound early control of highly pathogenic SIV by an effector memory T-cell vaccine. *Nature* 2011;473:523–527.

25. Hansen SG, Piatak MJ, Ventura AB, *et al.*: Immune clearance of highly pathogenic SIV infection. *Nature* 2013; 502:100–104.
26. Bilello JP, Morgan JS, Damania B, Lang SM, Desrosiers RC: A genetic system for rhesus monkey rhadinovirus: Use of recombinant virus to quantitate antibody-mediated neutralization. *J Virol* 2006;80:1549–1562.
27. Bilello JP, Manrique JM, Shin YC, *et al.*: Vaccine protection against simian immunodeficiency virus in monkeys using recombinant gamma-2 herpesvirus. *J Virol* 2011;85: 12708–12720.
28. Hansen SG, Sacha JB, Hughes CM, *et al.*: Cytomegalovirus vectors violate CD8+ T cell epitope recognition paradigms. *Science* 2013;340:1237874.
29. Hansen SG, Wu HL, Burwitz BJ, *et al.*: Broadly targeted CD8(+) T cell responses restricted by major histocompatibility complex E. *Science* 2016;351:714–720.
30. Masopust D, Ha SJ, Vezys V, Ahmed R: Stimulation history dictates memory CD8 T cell phenotype: Implications for prime-boost vaccination. *J Immunol* 2006;177: 831–839.
31. Thompson EA, Beura LK, Nelson CE, Anderson KG, Vezys V: Shortened intervals during heterologous boosting preserve memory CD8 T cell function but compromise longevity. *J Immunol* 2016;196:3054–3063.
32. Martins MA, Tully DC, Cruz MA, *et al.*: Vaccine-induced simian immunodeficiency virus-specific CD8+ T-cell responses focused on a single nef epitope select for escape variants shortly after infection. *J Virol* 2015;89:10820–10820.
33. Martins MA, Wilson NA, Piaskowski SM, *et al.*: Vaccination with Gag, Vif, and Nef gene fragments affords partial control of viral replication after mucosal challenge with SIV<sub>mac239</sub>. *J Virol* 2014;88:7493–7516.
34. Schmitz JE, Simon MA, Kuroda MJ, *et al.*: A nonhuman primate model for the selective elimination of CD8+ lymphocytes using a mouse-human chimeric monoclonal antibody. *Am J Pathol* 1999;154:1923–1932.
35. Gonzalez-Nieto L, Domingues A, Ricciardi M, *et al.*: Analysis of simian immunodeficiency virus-specific CD8+ T-cells in rhesus macaques by peptide-MHC-I tetramer staining. *J Vis Exp* 2016;118.
36. Schmitz JE, Forman MA, Lifton MA, *et al.*: Expression of the CD8alpha beta-heterodimer on CD8(+) T lymphocytes in peripheral blood lymphocytes of human immunodeficiency virus- and human immunodeficiency virus+ individuals. *Blood* 1998;92:198–206.
37. Parham P: Antigen recognition by T lymphocytes. In: *The Immune System* (Foltin J, Masson S, Ghezzi K, Engels A, Lawrence E, Jeffcock E, eds.) Garland Science, Taylor & Francis Group, LLC, New York, NY, 2009, pp. 125–154.
38. Cline AN, Bess JW, Piatak MJ, Lifson JD: Highly sensitive SIV plasma viral load assay: Practical considerations, realistic performance expectations, and application to reverse engineering of vaccines for AIDS. *J Med Primatol* 2005;34: 303–312.
39. Mudd PA, Martins MA, Ericson AJ, *et al.*: Vaccine-induced CD8+ T cells control AIDS virus replication. *Nature* 2012; 491:129–133.
40. Bimber BN, Dudley DM, Lauck M, *et al.*: Whole-genome characterization of human and simian immunodeficiency virus intrahost diversity by ultradeep pyrosequencing. *J Virol* 2010;84:12087–12092.
41. Yang X, Charlebois P, Gnerre S, *et al.*: De novo assembly of highly diverse viral populations. *BMC Genomics* 2012; 13:475.
42. Henn MR, Boutwell CL, Charlebois P, *et al.*: Whole genome deep sequencing of HIV-1 reveals the impact of early minor variants upon immune recognition during acute infection. *PLoS Pathog* 2012;8:e1002529.
43. Yang X, Charlebois P, Macalalad A, Henn MR, Zody MC: V-Phaser 2: Variant inference for viral populations. *BMC Genomics* 2013;14:674.
44. Allen TM, Sidney J, del Guercio MF, *et al.*: Characterization of the peptide binding motif of a rhesus MHC class I molecule (Mamu-A\*01) that binds an immunodominant CTL epitope from simian immunodeficiency virus. *J Immunol* 1998;160:6062–6071.
45. Loffredo JT, Friedrich TC, Leon EJ, *et al.*: CD8+ T cells from SIV elite controller macaques recognize Mamu-B\*08-bound epitopes and select for widespread viral variation. *PLoS One* 2007;2:e1152.
46. Loffredo JT, Maxwell J, Qi Y, *et al.*: Mamu-B\*08-positive macaques control simian immunodeficiency virus replication. *J Virol* 2007;81:8827–8832.
47. Masopust D, Picker LJ: Hidden memories: Frontline memory T cells and early pathogen interception. *J Immunol* 2012;188:5811–5817.
48. Damania B, Desrosiers RC: Simian homologues of human herpesvirus 8. *Philos Trans R Soc Lond B Biol Sci* 2001; 356:535–543.
49. Desrosiers RC, Sasseville VG, Czajak SC, *et al.*: A herpesvirus of rhesus monkeys related to the human Kaposi's sarcoma-associated herpesvirus. *J Virol* 1997;71:9764–9769.
50. Bosselut R, Kubo S, Guinter T, *et al.*: Role of CD8beta domains in CD8 coreceptor function: Importance for MHC I binding, signaling, and positive selection of CD8+ T cells in the thymus. *Immunity* 2000;12:409–418.
51. Cheroutre H: Starting at the beginning: New perspectives on the biology of mucosal T cells. *Annu Rev Immunol* 2004; 22:217–246.
52. Webster RL, Johnson RP: Delineation of multiple subpopulations of natural killer cells in rhesus macaques. *Immunology* 2005;115:206–214.
53. Jin X, Bauer DE, Tuttleton SE, *et al.*: Dramatic rise in plasma viremia after CD8(+) T cell depletion in simian immunodeficiency virus-infected macaques. *J Exp Med* 1999; 189:991–998.
54. Matano T, Shibata R, Siemon C, Connors M, Lane HC, Martin MA: Administration of an anti-CD8 monoclonal antibody interferes with the clearance of chimeric simian/human immunodeficiency virus during primary infections of rhesus macaques. *J Virol* 1998;72:164–169.
55. Okoye A, Park H, Rohankhedkar M, *et al.*: Profound CD4+/CCR5+ T cell expansion is induced by CD8+ lymphocyte depletion but does not account for accelerated SIV pathogenesis. *J Exp Med* 2009;206:1575–1588.
56. Alexander L, Aquino-DeJesus MJ, Chan M, Andiman WA: Inhibition of human immunodeficiency virus type 1 (HIV-1) replication by a two-amino-acid insertion in HIV-1 Vif from a nonprogressing mother and child. *J Virol* 2002;76: 10533–10539.
57. Deacon NJ, Tsykin A, Solomon A, *et al.*: Genomic structure of an attenuated quasi species of HIV-1 from a blood transfusion donor and recipients. *Science* 1995;270:988–991.

58. Kestler HW, Ringler DJ, Mori K, *et al.*: Importance of the nef gene for maintenance of high virus loads and for development of AIDS. *Cell* 1991;65:651–662.
59. Kirchhoff F, Greenough TC, Brettler DB, Sullivan JL, Desrosiers RC: Brief report: Absence of intact nef sequences in a long-term survivor with nonprogressive HIV-1 infection. *N Engl J Med* 1995;332:228–232.
60. Mariani R, Kirchhoff F, Greenough TC, Sullivan JL, Desrosiers RC, Skowronski J: High frequency of defective nef alleles in a long-term survivor with nonprogressive human immunodeficiency virus type 1 infection. *J Virol* 1996;70:7752–7764.
61. Alexander L, Weiskopf E, Greenough TC, *et al.*: Unusual polymorphisms in human immunodeficiency virus type 1 associated with nonprogressive infection. *J Virol* 2000;74:4361–4376.
62. Rud EW, Yon JR, Larder BA, Clarke BE, Cook N, Cranage MP: Infectious molecular clones of SIVmac32H: Nef deletion controls ability to reisolate virus from rhesus macaques. In: *Vaccines 92: Modern Approaches to New Vaccines Including Prevention of AIDS* (Brown F, Chanock RM, Ginsberg HS, Norrby E, eds.) Cold Spring Harbor Laboratory, New York, 1992, pp. 229–235.
63. Rud EW, Cranage M, Yon J, *et al.*: Molecular and biological characterization of simian immunodeficiency virus macaque strain 32H proviral clones containing nef size variants. *J Gen Virol* 1994;75:529–543.
64. Cranage MP, Whatmore AM, Sharpe SA, *et al.*: Macaques infected with live attenuated SIVmac are protected against superinfection via the rectal mucosa. *Virology* 1997;229:143–154.
65. Cranage MP, Sharpe SA, Whatmore AM, *et al.*: In vivo resistance to simian immunodeficiency virus superinfection depends on attenuated virus dose. *J Gen Virol* 1998;79:1935–1944.
66. Sharpe SA, Whatmore AM, Hall GA, Cranage MP: Macaques infected with attenuated simian immunodeficiency virus resist superinfection with virulence-revertant virus. *J Gen Virol* 1997;78:1923–1927.
67. Carl S, Iafraite AJ, Skowronski J, Stahl-Hennig C, Kirchhoff F: Effect of the attenuating deletion and of sequence alterations evolving in vivo on simian immunodeficiency virus C8-Nef function. *J Virol* 1999;73:2790–2797.
68. Loffredo JT, Valentine LE, Watkins DI: Beyond Mamu-A\*01+ Indian rhesus macaques: Continued discovery of new MHC class I molecules that bind epitopes from the simian AIDS viruses. *HIV Mol Immunol* 2006;2007:29–51.
69. Del Prete GQ, Scarlotta M, Newman L, *et al.*: Comparative characterization of transfection- and infection-derived simian immunodeficiency virus challenge stocks for in vivo non-human primate studies. *J Virol* 2013;87:4584–4595.
70. Kirchhoff F, Kestler HW, Desrosiers RC: Upstream U3 sequences in simian immunodeficiency virus are selectively deleted in vivo in the absence of an intact nef gene. *J Virol* 1994;68:2031–2037.
71. Pathak VK, Temin HM: Broad spectrum of in vivo forward mutations, hypermutations, and mutational hotspots in a retroviral shuttle vector after a single replication cycle: Deletions and deletions with insertions. *Proc Natl Acad Sci U S A* 1990;87:6024–6028.
72. Pulsinelli GA, Temin HM: Characterization of large deletions occurring during a single round of retrovirus vector replication: Novel deletion mechanism involving errors in strand transfer. *J Virol* 1991;65:4786–4797.
73. Klein F, Nogueira L, Nishimura Y, *et al.*: Enhanced HIV-1 immunotherapy by commonly arising antibodies that target virus escape variants. *J Exp Med* 2014;211:2361–2372.
74. Jost S, Altfeld M: Evasion from NK cell-mediated immune responses by HIV-1. *Microbes Infect* 2012;14:904–915.
75. Alter G, Heckerman D, Schneidewind A, *et al.*: HIV-1 adaptation to NK-cell-mediated immune pressure. *Nature* 2011;476:96–100.
76. Holzemer A, Thobakgale CF, Jimenez Cruz CA, *et al.*: Selection of an HLA-C\*03:04-restricted HIV-1 p24 gag sequence variant is associated with viral escape from KIR2DL3+ natural killer cells: Data from an observational cohort in South Africa. *PLoS Med* 2015;12:e1001900; discussion e1001900.
77. Carlson JM, Brumme CJ, Martin E, *et al.*: Correlates of protective cellular immunity revealed by analysis of population-level immune escape pathways in HIV-1. *J Virol* 2012;86:13202–13216.
78. Scully E, Alter G: NK Cells in HIV Disease. *Curr HIV/AIDS Rep* 2016;13:85–94.
79. Choi EI, Reimann KA, Letvin NL: In vivo natural killer cell depletion during primary simian immunodeficiency virus infection in rhesus monkeys. *J Virol* 2008;82:6758–6761.
80. Choi EI, Wang R, Peterson L, Letvin NL, Reimann KA: Use of an anti-CD16 antibody for in vivo depletion of natural killer cells in rhesus macaques. *Immunology* 2008;124:215–222.
81. Reeves RK, Gillis J, Wong FE, Yu Y, Connole M, Johnson RP: CD16- natural killer cells: Enrichment in mucosal and secondary lymphoid tissues and altered function during chronic SIV infection. *Blood* 2010;115:4439–4446.
82. Garcia KC, Scott CA, Brunmark A, *et al.*: CD8 enhances formation of stable T-cell receptor/MHC class I molecule complexes. *Nature* 1996;384:577–581.
83. Kern P, Hussey RE, Spoerl R, Reinherz EL, Chang HC: Expression, purification, and functional analysis of murine ectodomain fragments of CD8alphaalpha and CD8alpha-beta dimers. *J Biol Chem* 1999;274:27237–27243.
84. Wyer JR, Willcox BE, Gao GF, *et al.*: T cell receptor and coreceptor CD8 alphaalpha bind peptide-MHC independently and with distinct kinetics. *Immunity* 1999;10:219–225.
85. Cheroutre H, Lambolez F, Mucida D: The light and dark sides of intestinal intraepithelial lymphocytes. *Nat Rev Immunol* 2011;11:445–456.
86. Madakamutil LT, Christen U, Lena CJ, *et al.*: CD8alphaalpha-mediated survival and differentiation of CD8 memory T cell precursors. *Science* 2004;304:590–593.
87. Zhu J, Peng T, Johnston C, *et al.*: Immune surveillance by CD8alphaalpha+ skin-resident T cells in human herpes virus infection. *Nature* 2013;497:494–497.

Address correspondence to:  
 David I. Watkins  
 Life Science Tech Park  
 Department of Pathology  
 University of Miami  
 1951 NW 7th Avenue  
 Room 2340  
 Miami, FL 33136

E-mail: [dwatkins@med.miami.edu](mailto:dwatkins@med.miami.edu)